GEOFYSISKE PUBLIKASJONER

GEOPHYSICA NORVEGICA

VOL. XX NO. 9

RESULTS OF AURORAL OBSERVATIONS AT TROMSØ AND OSLO FROM THE FOUR WINTERS 1953—54 TO 1956—57

BY L. VEGARD, S. BERGER, AND A. NUNDAL

FREMLAGT I VIDENSKAPS-AKADEMIETS MØTE DEN 23DE MAI 1958

TRYKT MED BIDRAG FRA NORGES ALMENVITENSKAPELIGE FORSKNINGSRÅD

Summary. The present paper may be regarded as a continuation of papers by Vegard, where the observed facts are coordinated to a theory of solar terrestrial relationships, which explains a number of phenomena like the structure of the ionosphere, the zodiacal light, the comets, the solar corona and the electron ray bundles, which are neutralized by protons and probably other positive rays, and which produce the aurorae and allied cosmic-terrestrial phenomena. The theory is based on «the coronal effect of solar X-rays». In a foreword one of us (Vegard) describes the gradual development of this theory and the observational methods, which can be applied for its verification. The foreword will in this way also serve as plan for the investigations to be dealt with in this paper.

The paper is mainly based on auroral spectrograms taken at the Auroral Observatory, Tromsø and the Physical Institute, Oslo, during the four winters 1953/54—1956/57. The spectrographs have been described in previous papers (6, 9, 13). At Tromsø we used the «V» spectrograph characterized by fairly great dispersion and another «F» of extremely great light power. At Oslo we used the spectrographs we call (C) and (a).

The 15 spectrograms taken with the «V»-spectrograph were used for accurate wavelength determinations and interpretation of lines and bands. The proton velocities in the solar bundles were measured by means of the Doppler displacement of $H\beta$.

Accurate ionospheric temperatures were determined by the N_2^+1N bands, which gave distinct separation of the rotational components. Temperature measurements were also made by means of the «F»-spectrograms at Tromsø and C spectrograms at Oslo, at the height of about 100 km up to several hundred km, but no increase of temperature with altitude could be detected.

When the neutralized bundles enter the ionosphere the electric particles contained in the bundle are free to move and to be absorbed independently of each other, and this opens up a possibility for determining the nature of the particles and the height they reach.

The 139 «F»-spectrograms reproduced on the 5 plates II–a — II–e are mainly taken for the purpose of such an analysis. It was found that spectrograms taken near the bottom edge of the aurorae showed the characteristic features of spectrograms produced by electron rays, with strong bands and few lines. The red sequence, $\triangleleft n = 3$, of N_21P bands responsible for the red aurorae

of type (B) was very strong while the red OI-doublet was weak or absent and no trace of H-lines was observed.

The other group of «F» spectrograms corresponding to greater altitudes, however, showed the features characteristic of positive ray-excitation with more and stronger lines, weak or absent bands. The red OI-doublet producing the red aurorae of type (A) was greatly enhanced and the H-lines appeared.

These results confirm in a striking way the results previously found, that the enhancement of the red OI-doublet is not produced by electrons, but is due to the positive rays, mainly protons, contained in the bundle. The protons (and possibly other positive ions) have the ability to transfer the neutral O-atom from the $^3P_{2,1}$-states to the lowest metastable $^1D_2$ state. The enhancement of the red OI-doublet in accordance with this excitation process is seen to be very great. The effect of the positive ion excitation (proton excitation) is very pronounced in spectrograms taken at Oslo from aurorae appearing in great altitudes up to 600 km.

The excitation process, however, is a difficult problem, which still remains to be solved.

Preface

This communication, mainly based on auroral spectroscopy, is to be regarded as a continuation of papers recently published by Vegard, where the observed facts are seen in the light of a coherent theory which explains a number of solar and terrestrial phenomena, like aurorae, magnetic disturbances, the structure of the ionosphere, the zodiacal light, the solar corona and the ray bundles, which produce aurorae and magnetic disturbances by means of photo electrons from solar X-rays.

The theories have been gradually developed in the papers given in the list of references and a summary of them was recently given in a paper read at the conference on Chemical Aeronomy sponsored by the Geophysics Research Center, Cambridge, Mass. The meetings were held at Harvard University on the 25–28. June 1956. The paper is to be found on p. 22 in the proceedings of the conference edited by M. Zelekoff under the title: «The Threshold of Space», Pergamon Press, New York, London.

These theories date back to a paper published in 1916 (1) and have been developed, generalized and verified mainly by the study of aurorae and the spectral analysis of its luminescence. A short historical survey is given in connection with the list of references.

The solar soft X-rays of photon energy of 1 000–1 500 e. volts produce, by direct photo electric effect, the conductive atmospheric E-layer. The photo electrons, which are formed by X-rays on the way to the absorption limit just below the E-layer, form electron beams approximately neutralized by atmospheric ions, like O^+, N^+, O_2^+, N_2^+. The distribution of the electron concentration will vary upwards and produce reflecting maxima in the form of the F_2-layers.

The same soft X-radiation produces photo-electrons in the solar atmosphere and *electron bundles neutralized by positive solar ions of great specific charge and abundance (preferably protons) add up to form the solar corona around the sun.*

It is now of the greatest significance that the isolated solar bundles, which produce the aurorae and the more prominent polar magnetic disturbances, have essentially the same structure as the streamers of the solar corona.

The essential difference is that the X-rays, which produce the auroral bundles, are emitted from comparatively narrow sunspot areas, where the matter pumped up through the «sunspot activity» is highly ionised, and produces X-rays of photon energy which is usually more than 10 times greater than that of the coronal X-rays.

The photo-electrons from a limited area are mainly directed away from the sun's surface through the action of the local fields at the sunspots, and the mutual electromagnetic attraction between the streamers helps to concentrate the cross section of the bundles by an automatic focussing effect.

Thus the neutralized bundles, which produce the aurorae, are merely to be considered as a specially intensive form of solar coronal streamers, with a range sufficiently great to be driven into the sphere of influence of the magnetic field of the earth.

As the auroral streamers come down to altitudes of 100 km and even lower, the electrons and the primary sunspot X-rays may have energies amounting to 100.000 e.V. and sometimes much more.

Thus by studying the aurorae, their distribution in time and space, and their spectral composition under various conditions, we are able to test and verify by observations some of the most essential consequences of our auroral theory. In other words, we may prove that the aurorae are caused by bundles of electrons, produced by fairly energetic solar X-rays, and electrostatically neutralized by positive ions (protons) from the solar atmosphere.

These experimental results can then, with certain modifications, be transferred to the streamers of the solar corona. *This involves the important consequence that the radial distribution of matter in the corona is governed by these radiant processes and not essentially by extremely high temperatures.*

The verification of the consequences to be drawn from the constitution and properties of the neutralized bundles has been done more or less qualitatively, and, on account of the great variability of the proton flux and of the relative intensity of the H-lines, we have often to take our refuge in statistical methods. It is therefore of importance to base our investigations on a great number of observational data. It is also very important to take spectrograms of well defined types and observational conditions, and to improve the methods and the experimental equipment.

When the solar bundle enters into the atmosphere, there will be plenty of ions, and the electrons, protons and possibly other positive ions are no longer tied up with the condition of electrostatical neutralization, but are free to move and to be absorbed independently of each other. The height at which a particle stops will be determined by the law of absorption it has to follow.

This is a matter of great importance, because it enables us to identify and analyse the properties of the positive rays which have been used to neutralize the stream of photo-electrons emitted by a limited source of X-rays on the sun.

We have already been able to show that the lower limit of an aurora which is fixed by the absorption limit (h_e) of the photo-electrons is well separated from the protons, reaching down to a height (h_p) of the protons which is greater than (h_e). Thus there is an interval (h_p—h_e) where the spectrograms are typical for electron-excitation. That means that they have strong red nitrogen bands responsible for the red aurora of type (B), and a very weak red OI doublet.

From greater altitudes the auroral spectrograms show the features typical for positive ray excitation with great intensity of the red OI-doublet, the enhancement of which is responsible for the red aurora of type A, and the H-line usually appears at higher altitudes.

Spectrograms from different altitudes have shown that the protons, and probably other positive ions, have a specific ability to transfer the neutral oxygen atoms from the ground states OI ($^3P_{2,1}$) to the OI ($^1D_2$) state. This shows that the separation of the elements of the neutralized bundles can give results of great physical significance.

Following these procedures for the study of spectral types and their excitation at various altitudes, we have already found that the great variability of the relative proton flux or of the proton velocity relative to that of the electrons in the bundle, corresponds to a great variability in the excitation processes and in the spectral composition of the auroral luminescence.

In the present and previous communications (12, 13, 14) a great deal of work has been devoted to these problems and they call for much research work in the future. Thus it will be very important to apply experimental methods, which enable us to fix the exact position in space, which corresponds to a certain point or line on an auroral spectrogram and to register variations with altitude of auroral features.

One procedure which can be used with advantage, is to throw a picture on the slit of a spectrograph with great light power from a fairly quiet auroral display, in such a way that a vertical line of the aurora on the picture is parallel to the slit. In the interval of exposure parallactic photographs from two stations ought to be taken, by means of which the altitude along a spectral line can be determined.

The neutralized bundles, which take perhaps a day or more on their way from sun to earth, is not the only way in which the X-rays influence the atmosphere of the earth. The X-rays will leave the source of the sun with the velocity of light, and they will produce effects on the dayside of the atmosphere of the earth similar to those responsible for the solar and terrestrial corona.

The much more penetrating X-radiation emitted from the sunspot region (solar flares) produces a similar system of ionised layers like those of the ionosphere, but with the difference that the one corresponding to the E-layer is situated lower down in the atmosphere and is identical with that which is called the D-layer. On their way down to the bottom of the D-layer, the sunspot X-rays produce photo-electrons, which will be rapidly absorbed in the downwards direction, but have a rapidly increasing mean free path towards greater altitudes. They will form a similar system of neutralized photo-electron bundles like those which led to the formation of the F_2-layer above the E-layer. This formation of photo-electrons by the sunspot or solar flares — X-rays, will be going on from the extreme upper limit of the atmosphere to just below the D-layer.

On account of the much greater velocity and energy the sunspot X-rays (during flares) must considerably increase the extension of the terrestrial corona, and as the electron rays accompanied by positive atmospheric ions will pass over to the night-side, it is to be expected that the sunspot X-rays will increase the intensity, extension and height of the zodiacal light.

From analogy we have reasons to expect that the electron emission caused by the sunspot X-rays in the earth's atmosphere, will produce conductive layers similar to the F_2-layers. These atmospheric photo-electrons should have about the same energy as the electron bundles passing down to the bottom edge of aurorae. This energy may vary between say 10.000 to about 200.000 electron volts. The photo-electrons produced in our atmosphere by the sunspot X-rays form conductive layers analogous to the F_2-layers, they may be found lower down in the atmosphere but above the D-layer. The layers belonging to the D-system we may call D_0 and D_1, D_2 — where D_0 corresponds to the E-layer, and D_1, D_2 — to the F_2-layers. The height of the D-layers will vary with the X-ray energy, and there may be a great chance, for the layers D_1, D_2 — to be situated near the height of the ordinary E-layer, and thus account for the appearance of «sporadic E».

The formation of a coronal structure through photoelectric effect of solar X-rays is a very complicated process from a strictly mathematical point of view, although it can be clearly followed and deduced by direct physical reasoning from its start with X-rays to the resulting corona. It might therefore be convenient to call this important cosmical process: *The coronal effect of solar X-rays.*

The emission of X-rays is a universal property of stars, as far as we can assume, that vortex motions take place and bring highly ionized matter up to the surface. Thus all celestial bodies, which are surrounded by an atmosphere and hit by sufficiently strong X-rays, will develop a coronal structure. This includes e. g. stars, planets and comets exposed to X-rays from the sun or from a star.

Oslo, April 1958. *L. Vegard.*

1. The instrumental equipment. The auroral spectrograms to be dealt with in this paper were taken with glass-spectrographs. At the Tromsø observatory we used the two big spectrographs «V» and «F» and a small one (α), at Oslo two small spectrographs (C) and (a). The spectrographs (a) and (α) are practically identical and they were used to obtain comparable spectrograms for the study of the variation with latitude of the relative intensity of H-lines (11).

The light power and scale values in Å/mm are given in table 1.

Table 1. *Scale value (Å/mm).*

λ	«V», F:1.2	«F», F:0,65	C, F:0,95	a, F:2.0
4000	40	77	100	121
6000	188	395	550	665

2. Spectrograms obtained by the 4 spectrographs during the four winters from 1953/54—1956/57. The «V» spectrograph, which has the greatest dispersion was used first of all for an accurate determination of wavelength of lines and bands and their interpretation. For this purpose it was very important to adjust the instrument so as to obtain sharp lines. Applying a narrow slit, good adjustment and careful automatic temperature-regulation, we obtained very sharp lines throughout the spectrogram.

With this instrument we had to use long exposures. As a rule they lasted many days or even weeks.

The «V» spectrograms taken in this way gave also good conditions for the determination of the distribution of proton velocities by means of the Doppler-effect of H_β and of the ionospheric temperature by means of the (N_2^+ 1N) bands. In the case of the bands 4278 and 3914 the rotational components were fairly well separated.

The «V» spectrograms are reproduced on the plates I–a and I–b.

The «F»-spectrograph was used for the study of the variations, which were shown in the spectral composition of auroral luminescence under various circumstances and observational conditions. In this case the photographic reproduction of the spectrograms is very essential for the estimate of the results.

In the study of variations it is very essential that we can obtain spectrograms which correspond to a somewhat well defined situation. It is therefore a matter of importance that the great light power of the «F» spectrograph facilitates the use of short exposure.

The instrument makes it possible to take a number of spectrograms in rapid succession followed by an intensity scale on the same plate. Intensity-scales taken with a light source of known spectral intensity distribution enable us to compare intensities from different spectral regions.

The series of auroral spectrograms taken with the «F» spectrograph at Tromsø are reproduced on the 5 plates: II-a, II-b, II-c, II-d and II-e. For the estimate of the variational effects the explanations given for each spectrogram are very essential.

By means of the Oslo spectrograph (C), which is of higher quality and has a greater dispersion and much greater light power than the (a) spectrograph, we have obtained a considerable number of interesting spectrograms which are reproduced on plate III. Each plate is provided with an «explanation», which is placed in such a way that each spectrogram can be compared directly with the explanation.

Table 2. *Results from 4 «V» Spectrograms on Pl. I.*

4		7		11		12		Prev. obs.	Interpretation
λ	I	λ	I	λ	I	λ	I		
3914		3914		3914		3914		3914	N_2^+ 1N(o—o), S.R.(1—18)
				92.4				92.6	
95.7				94.8	1.6	94.4	1.3	95.2	NI(94.4) NII(95.0)
98.3	3.3	97.5	2.6	97.5	2.4	97.1	2.6	97.3	2P(1—4)
				4033.6				4033.1	OII(33.2) NI(33.6)
				40.7				41.2	NII(41.3) OII(41.3)
									NOβ (0—12)
				51.3		4050.0		51.5	
4058.5	3.	4058.5	2.3	58.5	2.4	57.8	2.4	58.5	2P(0—3)
		64.6		65.2		65.5		64.9	S.R. (3—20)
		71.7	0.4	71.0		72.0		70.5	OII(69.9, 69.6)
		74.3	0.3	75.4				75.9	OII(75.9)
		77.6						79.1	OII(78.9)
		86.4	0.3					86.4	OII(87.1)
				89.3				89.7	OII(89.3)
		96,7		96.3		97.1		97.7	OII(97.2, 97,3)
		4101.7		4101.0				99.7	2P(7—11) NI(99.9, 01.7)
				09.3		4109.4		4109.4	OII(10.2) NI(10.0)
									NII(10.0)
				22.6				21.0	OII(21.5, 20.6, 20.3)
						31.5		30.3	OII(29.3) NI(29.2)
4139.7		40.3	0.2	40.3		40.4		40.1	N_2^+ 1N(4—5)
		52.1						52.0	NI(51.5)
						64.0		64.0	NI(64.8) S.R.(3—20)
				67.4				67.5	NaI(67.8)?
		69.8	0.4					69.0	OII(69.3)
72.5		72.7		71.8				71.5	NII(71.6) V.K.(3—14)
									N_2^+ 1N(3—4)
		76.4	0.3	74.9		74.8		76.2	NII(76.2)
				80.3				80.2	NI(80.0) NII(79.7)
		85.6	0.3			84.8		85.1	OII(85.5)
89.4		90.2		88.5	0.6			89.7	OII(89.8)
93.8		95.1				93.7		93.5	OI(92.5) NI(93.5)
99.4	1.5	4200.6	1.–	98.1	1.2	99.4	1.4	99.7	N_2^+1N(2—3) 2P(2—6)
4205.0		05.3		4204.2		4204.3		4205.1	NI(05.7)
4211.9		4212.1		4210.3	0.5	4212.2		4211.6	NI(13.0, 09.1)
		15.7	0,4	15.1	0.6			15.1	NI(15.9, 14.7) NOβ(2—14)
16.9						17.0		17.6	OI(17.1)
35.2	6.9	36.0	11.2	36.1	8.7	36.1	11.6	36.2	N_2^+1N(1—2),NII(37.0,36,9)
41.0		42.1	0.4	41.2	0.9	41.1	1.2	41.5	NII(41.8)
76.8		77.0		77.5		76.7		78.0	N_2^+1N(0—1)
91.1	0.7	92.4	0.2					92.2	OII(92.1), NOβ(0—13)
94.4	0.7			96.0				94.4	OII(94.7), S.R.(1—20)
		4303.3		4303.4		4304.0		4304.1	OII(03.8), NOβ(3—15)

Table 2. Continued.

4		7		11		12		Prev. obs.	Interpretation
λ	I	λ	I	λ	I	λ	I		
		16.7	0.3	16.3				17.8	OII(17.7, 17.2) NI(17.7)
4319.0	0.7	18.7	0.3	18.5		19.8		19.2	OII(19.9) V.K.(1—13)
		21.8	0.3	20.8				21.3	NI(22.0)
		30.7	0.3					31.3	OII(31.8, 31.4)
35.1	0.7	35.8	0.4	33.9		35.3		34.5	OII(34.2)
42.7	1.6	43.5	1.0	42.6	1.0	43.0	1.0	43.8	OII(43.4, 42.8) 2P(0—4)
		47.6		46.8	0.6	47.0		46.7	OII(45.6, 44.3)
		50.5	0.4	50.3	0.8	50.6	0.9	51.0	OII(51.3)
57.7		57.6	0.3	57.7	0.6	57.5	1.6	58.0	OII(58.5, 57.3) NI(58.3)
67.7	1.3	68.5	1.5	68.1	2.1	67.7	2.6	68.3	OI(68.3)
78.7		79.4		78.6				78.8	OII(78.4)
		4412.0		4410.9				4411.4	S.R.(9—25)
4415.1	1.1	15.2	0.9	14.0	1.3	4414.9	1.4	15.1	OII(14.9)
22.6	0.8	23.3	1.0	21.6	0.6	23.0		22.6	S.R.(5—23)
27.6	0.7	26.9	0.5	26.0	0.7	28.6		27.3	NII(27.2)
32.9	0.9	32.6	0.6	31.2	0.8	33.7		32.6	NII(31.5, 32.7, 31.8)
				46.0				46.0	V.K.(0—10)
				48.2				48.7	NII(47.0)
67.7	0.7	65.3		64.9		65.4		66.0	OII(67.8, 66,3, 65.5) NII(65.5)
74.4		76.5		75.1				75.7	OII(77.9, 76.1) NII 77.3)
		83.5		83.6				82.8	OII(82.9) NOβ(2—15)
84.9	0.9	84.9				85.5		84.6	NI(85.1) N_2^+1N(5—7)
		87.0	0.4						
		89.7		88.4	0.7	88.4		88.2	OII(88.2, 87.7) NII(88.2)
		4501.8						4502.6	S.R.(1—21)
		10.4		4510.3				10.3	S.R.(6—24)
4515.8		15.1						14.8	N_2^+1N(4—6)
31.3	0.7	31.8	0.5	29.8	0.7	4532.5	0.6	30.8	NII(30.4)
54.2	0.7	52.2	0.4	51.2	0.6	53.3	0.7	53.1	N_2^+1N(3—5) NI(54.2, 53.4)
73.1	1.1	71.8	0.5	71.5	0.8	73.1	0.6	73.5	2P(1—6), NOβ(3—16)
		89.7	0.4	89.6	0.6			89.2	OI(89.9, 89.0)
91.2	0.9	94.4				90.9	0.7	91.8	OII(90.9), NO*b*(3—16)
4600.2	0.8	99.4	0.3	97.8	0.6	4600.1	0.6	4600.1	N_2^+1N(2—4)
08.8		4607.1	0.3	4608.7	0.4	08.9	0.5	09.6	OII(10.1, 09.4) NII(09.4)
		13.0						14.6	OII(13.9) 'NII(13.7)
21.6		20.3				20.6	0.5	22.4	OII(21.3), NII(21.4)
31.8	1.1	29.7	0.6	30.9	0.8	29.8	1.2	31.3	NII(30.6)
41.8	1.9	41.2	1.1	43.0	1.4	41.8	1.6	42.3	OII(41.8)NII(43.1)
51.3	4.6	51.0	4.6	51.3	4.6	51.3	4.6	51.2	N_2^+1N(1—3), NI(51.1) OII(50.9)
62.6	0.9	61.7		60.9	0.6	61.4	0.8	61.8	OII(61.7) NI(60.0)
79.0	1.1	77.6	0.3	76.9	0.8	78.9	0.9	77.4	OII(77.0, 76.2), NII (77.9, 75.0)

Table 2. Continued.

4 λ	4 I	7 λ	7 I	11 λ	11 I	12 λ	12 I	Prev. obs.	Interpretation
4709.6		4707.7		4707.0		4710.6		4709.1	N_2^+1N(0—2)
		22.9	0.3	20.5		21.7		20.6	NII(21.6, 18.4)
		69.3		68.3	0.5	69.3		68.0	
		75.3						73.3	OII(73.8, 72.9, 72.5)
		79.0						78.0	NII(79.7)
						83.3		82.5	NII(81.2)
		4803.3						4801.9	OI(03.0, 02.0, 01.8)
		17.9						16.3	S.R. (2—23)
		35.5		4833.9	0.5			35.5	V.K.(2—15), S.R. (11—28)
		38.6						38.0	NI(37.8)
		46.0				4846.2		45.5	NI(47.4)
		55.6		57.3	0.7			57.0	OII(56.8)
		60.3		61.7		62.5		61.4	Hβ
		90.7		92.2	0.6			90.1	OII(90.0) NOβ(3—17)
		96.8				96.1		96.4	NII(95.2)
		4900.7						99.2	V.K.(16—18)
4910.3				4913.3				4913.3	NOβ(3—17)
		35.1		32.2		4936.2		34.7	NI(35.0)
64.4	1.2	64.1		67.0				66.9	OI(68.8, 67.9, 67.4)
		80.7						80.2	OI(79.6)
97.1	1.4							98.7	NII(97.2)
		5000.6		5000.7	1.9			5001.5	NII(01.1)
		03.1		03.6	1.9	5004.1	1.5	02.9	NII(02.7)
5005.6	2.2	05.8	1.1					04.8	NII(05.1)
		10.5						10.2	NII(11.2, 10.6)
						5138.5		5139.5	NI(40.8)
		5199.5	0.9	5199.3	1.8	99.3		99.5	NI($^4S_{3/2}$—$^2D_{5/2}$) (NI(97.1)
		5202.5						5201.0	NI($^4S_{3/2}$—$^2D_{3/2}$) NI (01.6)
5230.7	2.7	28.6	1.3	5227.5	2.8	5229.7		28.2	N_2^+1N(0—3), NI(27.0)
				51.3	1.5			50.0	S.R. (4—26)
		64.3	1.0	62.9				63.0	S.R.(9—29)
				70.6	2.0			70.4	1P(15—10), NII(72.6)
				83.7	1.8				O_2^+1N(2—0)
		89.2				87.9	2.5	91.6	O_2^+1N(2—0), NI(92.8) S.R.(7—28)
		5320.0						5321.2	1P(13—8), NII(21.0)
		5433.3						5430.9	1P(10—5)
				5463.2		5462.3		61.7	NII(62.6), 1P(9—4)
		66.8						67.0	V.K.(3—17)
		5513.5		5512.8	1.0			5511.6	OI(12.7)
		44.1						43.9	1P(7—2), NII(43.5)
		52.0		52.8	1.1			51.5	1P(7—2), NII(52.0) NI (51.4) S.R.(7—29)
		56.2				5554.3		55.0	1P(7—2), OI(54.9)

Table 2. Continued.

4		7		11		12		Prev. obs.	Interpretation
λ	I	λ	I	λ	I	λ	I		
5577		77		77		77		77	OI($^1D_2$—$^1S_0$)
		95.0	2.1	97.6	3.3			96.9	O_2^+1N(1—0), 1P(6—1)
5604.8	3.0	5604.4	2.1	5603.3	3.2			5601.8	O_2^+1N(1—0), NI(04,4, 00,5), V.K.(0—15)
		11.3	1.9	11.8	3.0	5608.3	2.6	09.8	O_2^+1N(1—0), 1P(5—0), NI (11.3)
14.6	3.0							16.7	O_2^+1N(1—0), 1P(15—11) NI(16.5)
23.9	3.1	19.9	1.6	23.5	2.4	24.1	1.8	21.3	O_2^+1N(1—0), 1P(5—0), NI (23.0, 18.0) S. R. (12—26)
		5627.5	1.2					5625.8	O_2^+1N(1—0)
5630.2	1.9	30.0		5629.0	2.2	5632.2	1.3	30.3	O_2^+1N(1—0), 1P(5—0)
67.0		66.0	0.5	66.6	1.1	67.1	0.9	66.5	NII(66.6)
79.5	1.9	79.5	1.0	80.9	2.3	81.8	2.1	79.8	NII(79.6, 76.0)
		5712.4		5712.5	0.7			5710.4	NI(10.7), NII(10.8) 1P(13—9)
		24.7				5726.0		22.1	OI(20,6), 1P(12—8), S.R.(6—29)
				32.4	0.9			31.3	NII(30.7), OI(31.1), IP(12—8)
				47.6	1.0	45.7		45.6	NI(47.3), NII(47.3), 1P (12—8), S. R.(6—25)
5753.6		54.4		56.3	1.1	54.7		53.8	NI(52.7),1P(12—8), N_2^+1N (1—5), NII($^1D_2$—$^1S_0$)
						69.6		69.2	NI(72.8, 68.6)
80.6				79.0		78.2		78.3	NI(81.7), V.K. (5—19)
				89.5		89.3		91.8	NI(93.5, 90.4)
		5808.1		5807.5				5806.9	1P(11—7)
		25.4						27.4	NI(29.6)
5834.1	1.2	33.9	0.6	34.5	1.7	5830.7	1.2	31.3	1P(10—6), NI(34.8)
		37.6						36.8	1P(10—6), S.R.(1—26)
				44.0				43.9	1P(10—6), NI(41.1)
56.5	1.4	57.6		54.4	1.3	55.5	1.2	52.1	1P(10—6), NI(54.1)
		69.3						70.3	N_2^+1N(0—4)
79.0		77.5		74.9	1.5	79.4	1.6	77.9	
85.5		84.1		83.3				87.6	1P(9—5)
92.2	2.0	92.3	5.7	91.4	4.7	94.8	2.4	92.2	Na D_1D_2, 1P(9—5)
5906.6	1.3	5909.7				5908.7	1.2		1P(9—5)
		26.9		5929.0	1.2			5927.1	NII(27.8), NI(27.5)
35.2	1.3	34.8	0.7	35.7		37.4	1.2	36.9	1P(8—4)
60.4	2.4	58.3	1.6	60.8	2.2	60.2	2.4	58.9	NI(58.8), NII(60.9) 1P(8—4)
77.3	3.3	76.4	2.1	77.8	2.7	74.9	2.6	76.6	O_2^+1N(0—0)
				81.9					O_2^+1N(0—0)

4	
λ	I
94.7	3.5
6006.9	3.6
13.9	3.4
22.0	
47.4	1.9
61.4	1.9
69.6	2.2
98.7	
6111.8	2.8
18.6	
30.1	2.8
58.4	2.3
74.5	1.6
85.8	1.3
6226.4	
36.9	
51.8	
74.3	1.9
6300.3	
21.2	
62.6	
81.3	
93.3	
6401.8	
6416.7	

Table 2. Continued.

4 λ	4 I	7 λ	7 I	11 λ	11 I	12 λ	12 I	Prev. obs.	Interpretation
		84.3						84.2	O_2^+1N(0—0)
		88.6		87.4				87.1	O_2^+1N(0—0), NI(87,5)
94.7	3.5	93.1	2.3	93.1	3.0	93.1	2.9		O_2^+1N(0—0), 1P(7—3), OI (91.3)
6006.9	3.6	6006.1	2.5	6008.8	3.1	6005.5	3.0	6008.0	NI(08.4), 1P(7—3)
13.9	3.4	12.8	2.0	14.2		12.6	2.9	12.4	1P(7—3), NI(12,0), S. R. (6—30)
22.0		24.2		24.9		23.4	1.5	24.6	O_2^+1N(0—0), S.R.(3—28)
47.4	1.9	46.2	1.1	43.5		44.2	2.2	44.2	OI(46.5, 46.2), NI(44.8)
		51.2		49.0	2.1			49.2	1P(6—2)
61.4	1.9	62.6		64.7		58.3	1.8	60.9	1P(6—2), NI(61.9)
69.6	2.2	70.2	0.9	71.9	1.8	66.3	1.8	70.1	1P(6—2), NI(69.0)
98.7		98.3	0.4	96.1		96.7	1.5		1P(5—1)
		6103.2	0.8	6103.6					1P(5—1)
6111.8	2.8	12.6	1.8	12.5	2.7	6108.4	2.6	6109.8	1P(5—1), N_2^+2N(3—0)
18.6		21.2		21.5		17.7		19.0	S.R.(7—31)
						25.2	2.6	26.9	1P(5—1), V.K.(7—21), S.R. (4—29)
30.1	2.8	31.7	2.0	32.7	2.9	35.2	2.5		NII(36.9) N_2^+2N(3—0)
		54.2				54.3	2.4	55.1	1P(4—0)
58.4	2.3			58.5	2.4	58.4		57.1	1P(12—9) (4—0), OI(56.0, 56.8, 58.2)
		62.1	1.8					63.3	1P(12—9) (4—0)
				72.8	1.4				1P(12—9) (4—0)
74.5	1.6	74.4						74.9	1P(12—9), S. R. (1—27), NII(73.4)
		79.9				82.0	1.3		1P(12—9) (4—0)
85.8	1.3			86.5				84.1	1P(12—9) (4—0)
6226.4		6225.0				6227.4		6222.0	NI(24.1), S.R. (5—30)
36.9		40.6	1.0	6236.4	0.9	39.6	0.8	38.8	NI(37.5), 1P(11—8)
51.8								52.0	
		62.6	0.8	60.4	0.8	59.4	0.6		
74.3	1.9	73.7	1.3	69.9	1.6	71.3	1.8	71.8	NI(72.8), S.R.(2—28), N_2^+2N(4—1)
6300.3		6301.5		6301.1		6302.3		6300.3	OI 2P^4($^3P_2$—$^1D_2$) N_2^+2N(4—1)
21.2		23.9		22.5		19.8		20.7	1P(10—7), NI(21.7)
		29.8				28.4		29.6	1P(10—7)
62.6		63.8		63.8		63.2		63.8	OI2P^4($^3P_1$—$^1D_2$)
81.3		81.1		83.1		80.4		81.4	NI(78.0), O_2^+1N(0—1), 1P (9—6)
93.3		92.3		94.3		90.7		91.9	
6401.8						99.2		98.0	O_2^+1N(0—1), 1P(9—6)
		6403.5		6405.3					O_2^+1N(0—1)
6416.7		16.3		20.7		6416.7		6417.0	NI(17.1), O_2^+1N(0—1)

Table 2. Continued.

4 λ	4 I	7 λ	7 I	11 λ	11 I	12 λ	12 I	Prev. obs.	Interpretation
37.1						35.4		38.6	NI(37.3)
		40.2		42.7				42.0	1P(8—5)
		52.7				53.7		56.0	OI(53.6, 54.5) 1P(8—5)
						62.5		61.8	1P(8—5)
64.8		67.0						68.0	1P(8—5)
79.1						76.9		79.3	NII(82), N_2^+2N(5—2)
		83.1		86.9				85.5	NI(84.9)
						6503.3		6506.1	NI(06.), NII(04.9)
6510.5		6509.6						11.9	NI(10.3)
		19.1							1P(7—4)
		26.1				24.6		24.9	NI(28.4), 1P(7—4), NII (22.3)
						35.6		32.4	1P(7—4), NII(33.0)
42.4		46.5		46.6		45.2		43.0	1P(7—4)
		60.0						60.5	Hα
						80.0		83.3	NII(83.4), forbidden?
6619.6				6616.7				6616.8	1P(6—3)N_2^+2N(6—3)
						6658.8		55.2	NI(56.6, N_2^+2N(6—3)
68.6		6669.5		71.6				69.0	
						75.6		74.5	1P(5—2)
				91.7				93.5	1P(5—2)
		98.9				98.4			
				6748.2				6748.5	1P(4—1)
				63.3					1P(4—1)
				83.0				80.8	1P(4—1)

3. Results obtained with the «V» spectrograph. During the last four winters we have obtained 15 «V» spectrograms which are reproduced on the plates I–a and I–b. In all cases the lines appear sharp. In most cases only the somewhat strong well known features appear, but these are very appropriate for temperature determinations. Wavelength measurements have only been carried out for the four strongest spectrograms Nos. 4, 7, 11 and 12 on the plate. The results are given in table 2, which also includes the relative intensities (I) of the features, which are sufficiently strong and distinct for intensity measurements. The last wavelength column contains corresponding auroral features from previous observations (cfr. papers 6, 9, 13).

The determination of (λ) and (I) has been carried out by means of photometer curves, but in this case we have only put up those maxima, which correspond to features seen on the negative. For this reason, and because the present spectrograms do not show so many of the weakest feature, the number of lines and bands is smaller than it was given in papers (6, 9 and 13) for the same wavelength interval.

On the other hand a few features are found in the present wavelength table, which are not listed previously. In most cases this merely means, that a complex feature has been split up on account of the result of a narrow slit, a better adjustment and a careful temperature regulation.

The auroral features of table 2 are restricted to the spectral interval 3914–6780 and even in this interval a great number of auroral features appear which are too weak to be seen on the negative.

More complete tables derived from spectrograms containing more weak lines in the visible part and features in infrared and ultraviolet are listed and discussed in previous papers (6, 9, 13).

On account of the narrow slit and good adjustment and regulations, we ascertained that the atomic lines showed up very distinctly as compared with maxima due to the bands. The lines could therefore be accurately measured, but as regards interpretation the uncertainty of coincidences of several features comes in.

Apart from the yellow sodium doublet (D_1, D_2) and the H-lines H_α, H_β, H_γ only lines from neutral and singly ionized O- and N-atoms were observed on the «V»-spectrograms on plate I. The number of each group of these lines is given in table 3.

Table 3.

Symbol	OI	OII	NI	NII
Number	22	63	72	52

In the table 3 we have counted coincidences and multiplets.

In table 2 are listed the vibrational bands of the following systems:

The N_2 bands: N_2^+1N, N_2^+2N, Vegard–Kaplan bands,
N_2 1P and N_2 2P

O_2 bands: O_2^+1N, Schuman Runge (S.R.)-bands and NO_β-bands.

As not only the vibrational bands, but also the components of their fine structure have been listed, the table 2 is seen to contain a fairly large number of auroral bandfeatures.

Table 4 will give an impression of the band systems possibly observed on the «V» spectrograms.

Table 4.

Band system	N_2^+1N	N_2^+2N	N_2V.K.	$N_2$1P	$N_2$2P	O_2^+1N	O_2S.R.	$NO\beta$
Number Sequence	5	1	6	3	3	4	10	3
No Vibr. Bands .	16	4	9	19	6	4	22	7
Number Features	16	8	9	67	6	18	22	10
$\Delta n = v'-v''$	0, 1, 2, 3, 4,	3	10, 11, 12, 13, 14, 15	3, 4, 5	3, 4, 5	2,1,0–1	17, 18, 19, 20, 21, 22, 23, 24, 25, 26	12, 13 14

When the vibrational bands have no fine structure the number of the features and of the vibrational bands is equal. This should hold for the systems (N_2^+1N), (N_2^+V.K.), ($N_2$2P) and O_2S.R.-systems. The systems (N_2^+2N) and (NO_β) are known to form doublets. The ($N_2$1P)-system has a fine structure and on the present «V» spectrograms we have observed bands which show 4 to 5 maxima.

We must remember, however, that the spectrograms here dealt with only cover part of the auroral spectrum, and only a fraction of the weaker lines, which have been found on more strongly exposed spectrograms, particularly dealt with in paper (13).

4. Illustration of the spectrogram No 15 on pl. I, by means of the photometer curve. As seen from plate I–b the spectrogram No. 15 shows a fairly great

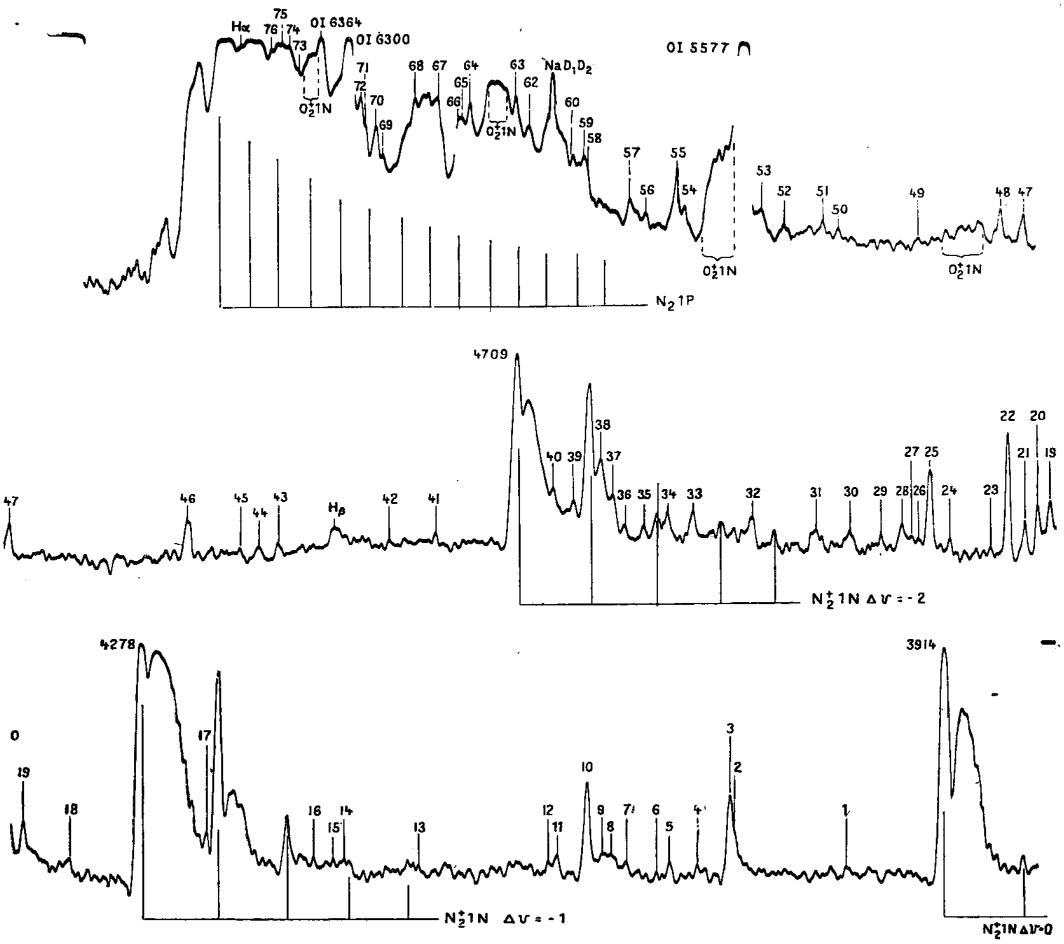

Fig. 1.

number of features, and it has been illustrated by means of a photometer curve taken with a Moll photometer. This curve is shown in fig. 1.

Some of the most prominent lines have been indicated by numbers from 1 to 76. The bands have been indicated by the band-symbols or by the wavelength of the strongest band-heads.

The wavelength (λ) corresponding to each number on the figure 1 is given in the table (5) shown close to the diagram. λ_p is the fourth figure of the wavelength λ_p from previously measured lines. $\triangle \lambda_p$ is the difference λ–λ_p.

The H_β-line with its Doppler effect is clearly seen. H_α-appears distinctly on the negative. In the reproduction and on the photometer curve, however, it is partly masked by the ($N_2 1P$)-bands.

The sodium doublet (D_1, D_2) appears strong and distinct.

The four sequences of (O_2^+ 1N) bands are seen very distinctly.

Line No. 47 is the forbidden NI doublet with a mean wavelength 5199, and it appears to be relatively strong. This agrees with the relatively strong H-lines, for as mentioned in previous papers there is reason to believe that the forbidden NI line (5199), and also other forbidden auroral features, are enhanced by increase of relative proton flux. (Cfr. papers: 10, 12, [13 p. 46, 47]).

5. The ionospheric temperatures determined by the R-branch of the bands (N_2^+1N) which appear on the «V»-spectrograms. With regard to the method used by the measurements of temperature in the auroral region by means of the intensity-distribution within the R-branch of negative nitrogen bands, we may refer to the papers 4b, 15 and 16.

As seen from the spectrograms reproduced on the plate I–a and I–b, the rotational components are well marked so rotational quant number and corresponding relative intensity can be found for each rotational component.

The temperature can be found in two ways which correspond to the following two equations:

$$T_m = 2{,}96\ (2\ K_m + 1) \qquad (1)$$

K_m is the rotational quant number corresponding to maximum intensity of the R-branch.

The temperature can also be derived from the equation:

$$\log_{10}\ (I_K/K) = -\ \varkappa\ (K + 1)K \qquad (2)$$

I_K is the intensity of the rotational component with rotational quant number K.

$$\varkappa = \frac{h^2 \log_{10} \varepsilon}{8\,\pi^2\,jkT_\varkappa}$$

k is Boltzmanns constant,

j the moment of inertia of the N_2^+ ion in the excited state.

This gives: $$T_\varkappa = \frac{1.286}{\varkappa}$$

Table 5. *Explanation to Diagram Fig. 1. giving Wavelengths and Interpretation of Spectral Features, which are clearly indicated on the Photometer curve from a «V»-spectrogram taken at Tromsø 24.1.57 to 4.3.57, reproduced on Pl. I—b.*

No	λ Plate 103a–E	λ_p	λ—λ_p	Interpretation
1	3954.3	5	— 0.7	OI (OII)
2	95.7	5	+ 0.7	NII (NI)
3	98.3	7	+ 1.3	N_2 2P(1—4)
4	4011.3	1	+ 0.3	NI
5	22.6	4	— 1.4	OII
6	27.9	6	+ 1.9	N_2 (OII)
7	41.5	1	+ 0.5	NII (OII)
8	48.2	8	+ 0.2	OII
9	52.9	4	— 1.1	OII
10	58.9	9	— 0.1	N_2 2P(0—3)
11	73.1	3	+ 0.1	OII (NII)
12	78.3	9	— 0.7	OII
13	4132.8	3	— 0.7	OII
14	71.8	1	+ 0.8	NII
15	77.6	6	+ 1.6	NII
16	86.5	5	+ 1.5	OII
17	4241.7	1	+ 0.7	NII
18	4318.5	8	+ 0.5	NI (OII)
19	43.1	4	— 0.9	N_2 2P(0—4) OII
20	50.6	2	— 1.4	OII
21	58.4	8	+ 0.4	NI (OII)
22	68.3	8	+ 0.3	OI
23	79.9	9	+ 0.9	OII
24	4403.4	3	+ 0.4	NOβ (1—14)
25	16.4	5	+ 1.4	OII
26	24.0	4	0.0	V.K. (2–14), S.R.(5–23)
27	27.5	7	+ 0.5	NII
28	33.4	3	+ 0.4	NII
29	45.6	8	— 2.4	NII
30	66.3	6	+ 0.3	OII
31	89.3	8	+ 1.3	OII
32	4532.4	30	— 0.6	NII
33	73.5	3	+ 0.5	$N_2$2 P(1—6)
34	89.6	90	— 0.4	OI (OII)
35	4608.5	9	— 0.5	OII
36	21.4	1	+ 0.4	NII (OII)
37	30.8	1	— 0.2	NII
38	42.1	2	+ 1.1	OII (NII)
39	62.2	2	+ 0.2	OII
40	78.5	8	+ 0.5	OII (NII)
41	4772.7	3	— 0.3	OI
42	81.0	2	— 1.0	NII

Table 5. Continued.

No	λ Plate 103a–E	λ_p	$\lambda—\lambda_p$	Interpretation
43	4914.5	5	— 0.5	N_2 2P(1—7)
44	32.4	2	+ 0.4	
45	54.7	5	— 0.3	OII
46	5003.4	3	+ 0.4	NII
47	5199.3	9	+ 0.3	NI
48	5229.4	8	+ 1.4	N_2^+1N(0—3)
49	5329.3	9	+ 0.3	OI
50	5436.5	6	+ 0.5	OI
51	63.8	2	+ 1.8	NII
52	5518.1	7	+ 1.1	$N_2$1P(8—3), OI
53	54.6	4	+ 0.6	$N_2$1P(7—2), OI
54	5669.2	6	+ 3.2	NII
55	81.2	0	+ 1.2	NII
56	5731.1	1	+ 0.1	NII (OI)
57	57.8	8	— 0.2	NI
58	5830.4	0	+ 0.4	NI
59	40.7	2	— 1.2	NI
60	60.1	9	+ 1.1	NI
61	5937.9	40	— 2.1	NII
62	61.7	2	— 0.3	NI
63	6047.8	7	+ 0.8	OI
64	63.0	2	+ 1.0	NI
65	71.2	1	+ 0.2	NI
66	6117.9	9	— 1.1	S.R.(7—31)
67	62.3	58	+ 4.3	OI
68	6227.1	4	+ 3.1	NI
69	42.2	3	— 0.8	NII
70	64.8	5	— 0.2	OI
71	75.1	3	+ 2.1	NI
72	6419.5	7	+ 2.5	NI
73	42.0	1	+ 1.0	NI
74	55.4	5	+ 0.5	OI
75	81.7	2	— 0.3	NII

If the distribution of intensities follows Maxwell's law and the rotational components were well separated, T_π ought to be equal to T_m. If the dispersion is so small that the rotational components overlap, or if the bands are partly over-exposed, T_m is usually too small and $T_\varkappa$ too great, and the mean value will usually come nearer the truth.

In the case of the N_2^+1N bands from the «V» spectrograms on plate I, the rotational components of the R-branch are nearly separated and usually one of the bands 4278 and 3914 has a suitable exposure for temperature measurements.

The results are given in table 6. It appears that the values of T_m and $T_\varkappa$ only show small differences. The ionospheric temperatures given in table 6 are in good agreement with those previously obtained.

Table 6. *Absolute Ionospheric temperatures from «V» spectrograms on Plates Ia and Ib.*

Plate I–a.

Band	No	1	2	3	4	5	6	7	8
4278	$T_\varkappa$	236	239	250	227	226	227	214	226
	T_m	224	202	254	231	231	241	182	209
3914	$T_\varkappa$				221	216	213	214	198
	T_m				196	216	209	196	231

Plate I–b.

Band	No	9	10	11	12	13	14	15	Mean Ia–b
4278	$T_\varkappa$	228	237	221	239	270	229		233.5
	T_m	246	224	202	206	224	196		219.4
3914	$T_\varkappa$	217	229	228	242		282	228	226.2
	T_m	216	238	209	216		286	224	221.5

Total Mean 225.3 K

÷ 47.7 C

6. The distribution of proton velocities in the ionosphere measured by means of Doppler displacement of H_β. By the motion through the ionosphere the protons are subject to the deviating force of the magnetic field of the earth. They will have a tendency to follow the magnetic lines of force, but usually the orbit of the proton will form an angle with the magnetic line of force, and form a screw line. The number of turns pro unit length will increase downwards. At a certain height it will take the form of a circle and return into space. On account of the absorption, the proton velocity gradually decreases. If our instrument is directed towards magnetic zenith the proton velocities will be greater towards the observer than in the opposite direction, and when the proton has captured an electron, it starts running in a straight line, which is the tangent to the orbit at the moment the proton was neutralized. The magnetic field of the earth will thus have the effect that the Doppler displacement will be greater towards decreasing wavelength values than in the opposite.

If, however, the axis of the collimator is directed perpendicular to the magnetic lines of force, the Doppler displacement should be nearly equal in both directions.

In the passage of the protons through the upper atmosphere, they will be subject to scattering, but the distribution of the proton velocities should be similar to that produced by the magnetic field.

In some previous papers we have seen that the Doppler displacement of the H-lines follows the rules here mentioned (cfr.papers 5(e), 6, 9, 13.)

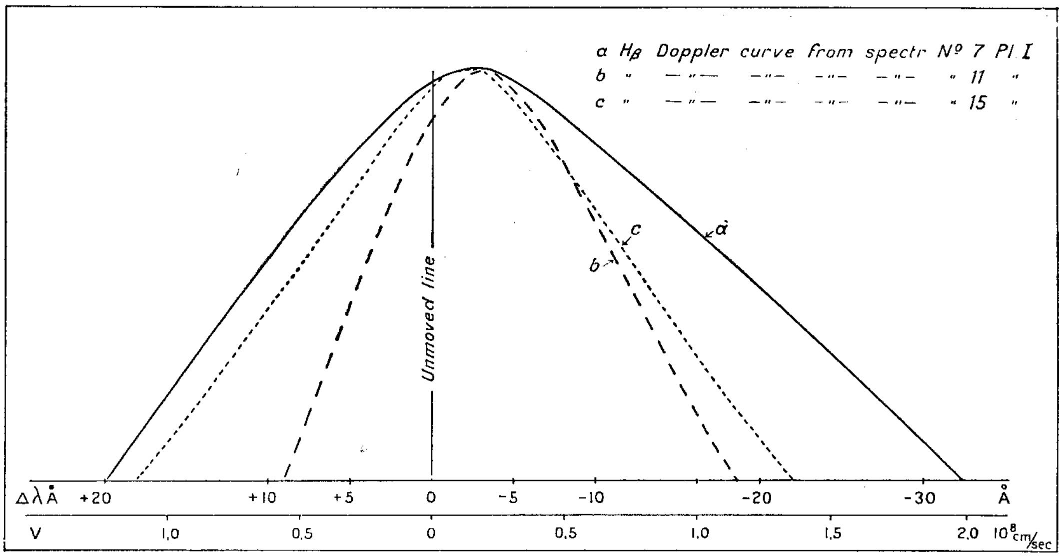

Fig. 2.

The velocity-distribution due to the influence of the magnetic field of the earth is most variable, but the distribution due to scattering might possibly be computed theoretically at any rate if the primary protons had a constant velocity and if the composition of the atmosphere was known as a function of altitude. But also the velocity distribution due to scattering is very complicated.

On the spectrograms on plate I–a and I–b only the spectrograms Nos. 7, 11 and 15 give a H_β-band sufficiently distinct for determination of the intensity distribution as a function of wavelength. The H_β-lines are also seen on spectrograms Nos. 9, 10–14, but they are too faint for photometric intensity measurements.

Smoothed curves of the Doppler bands of H_β were drawn on the photometer curves of the three spectrograms and shown on fig. 2, where the Doppler displacement $\triangle\lambda$ and the corresponding proton velocities are indicated.

The maximum velocities $(V_p)^-$ towards shorter waves and $(V_p)^+$ towards increasing λ are put up in table 7.

The maximum velocities thus found will usually increase with the photographic

Table 7. *Observed Proton Velocities.*

Sp. No.	Date	$(V_p)^-$cm/sec	$(V_p)^+$ cm/sec	Remarks
7	20.11.54—16.2.55	1.99 . 10^8	1.23 . 10^8	Tow. Magn. Eq. N.
11	30. 1.56—19.2.56	1.16 . -	0.56 . -	Various direct.
15	24. 1.57— 4.3.57	1.36 -	1.13 -	— —

density of the H-bands to a certain higher limit. The limit reached by V_p will change by the different auroral displays. It is found by laboratory experiments, that the intensity of H-lines from a Hydrogen canal ray bundle diminishes with increase of velocity, and it seems to vanish at velocities greater than about (3–4) 10^8 cm/sec (17).

The limit of the proton velocities in the solar electric ray bundles can be estimated by means of the absorption of protons in the atmosphere.

It may in this connection be mentioned that the H-lines appear to be absent at the lower part of aurora reaching down to altitudes smaller than say 105 km.

VARIABILITY EFFECTS STUDIED BY MEANS OF THE «F»-SPECTROGRAPH AT TROMSØ

7. Spectral variations of auroral luminescence resulting from the composition and properties of the neutralized bundles. Section B of paper (13) published in 1956 deals with the variations in composition of the auroral luminescence by means of «F»-spectrograms, which were obtained during the two winters 1951/52 and 1952/53, particular interest being paid to auroral spectrograms which might give information regarding properties and excitation capacity of the neutralized solar bundles.

Also during the four following winters until 1956/57 we have tried both at Oslo and Tromsø to take spectrograms, which were likely to give us information regarding the constitution and behaviour of the neutralized bundles.

In the following we are going to deal with consequences to be drawn from the constitution of the neutralized bundles and their verification by auroral observation.

As shown in previous papers (4, 10, 11, 12, 13, 14) an increase of the flux of positive ions will increase the mean distance from the aurorae to the magnetic axis point (cfr. papers 10, 11, 12, 13). This conclusion has been verified by comparing spectrograms taken at different latitudes e. g. Tromsø and Oslo (papers 10 and 11).

When a neutralized bundle passes into the atmosphere, the positive ions and the electrons will be free to move independently of each other. The range of the various constituents of the bundle and the height at which they stop, will be different.

By studying the spectrograms of the luminescence at various altitudes it might be possible to find effects from each type of particles originally contained in the bundle. As a rule the electrons will have the greatest range and be absorbed at a height (h_e) near the bottom edge of the auroral streamers. The protons (and other positive ions in the bundle) however, will stop at greater altitudes.

In order to observe the positive ions present in the bundle, they must either emit light of such wavelength that is is not absorbed by passing through the atmosphere, or they must produce other observable effects e. g. through their excitation of light of other particles. As part of the bundle in empty space, the protons do not emit the hydrogen lines. When the bundles pass into the atmosphere, and the protons are released, they gradually pick up electrons under emission of the hydrogen spectrum. This involves that the intensity of hydrogen lines along the auroral streamers first becomes noticable below a certain altitude. Then the H-line intensity gradually increases to a maximum usually near the height (h_p), where the protons are stopped. If the bundle carries other positive ions than protons, these are more highly ionised, and they can only be expected to emit light which will be absorbed by the passage through the atmosphere.

Such light might perhaps be observed from rockets reaching altitudes of the order of a hundred km or more.

In the case of ordinary aurorae with a bottom edge below say 105 km, the stopping height (h_p) of the protons is greater than (h_e) and there will often be a great height interval (h_p–h_e), where the auroral luminescence is excited by electrons only. This conclusion can be verified by comparing spectrograms taken near the bottom edge of the aurorae with such taken from greater altitudes. Such spectrograms from fairly great altitudes can e. g. be taken in a convenient way by directing the collimator towards magnetic zenith (cfr. paper 13 p. 44).

The spectrograms taken only near the bottom edge, will not as a rule, show any hydrogen lines, while those taken from greater altitudes with sufficient exposure almost without exception will show hydrogen lines, unless the height is so great that only a few protons have captured electrons.

In order to get a sensitive indicator for the appearance of H-lines, we have to use photographic plates, which are very sensitive to H_α. The fact that we are able to take spectrograms from auroral luminescence, which is excited by electrons is of great interest, because in many cases spectrograms are observed which are partly excited by the positive ions contained in the bundle, at any rate if the spectrum shows the features, which are typical for positive ray-excitations.

At altitudes above the stopping points of protons and other positive ions, we must expect to obtain spectrograms which show a great variability in the spectral composition. As we shall see such spectrograms show a great enhancement of the forbidden red doublet of OI (6300 og 6364) usually accompanied by the appearance of H-lines.

When the enhancement of the red OI-doublet is very great compared with other features in the spectrum, the aurora appears red (Red Aurorae of Type A). As the enhancement increases with altitude, we may sometimes observe auroral streamers which are merely red towards the tops of the rays.

The luminescence, which is emitted from the lower limit of ordinary aurorae, at altitudes below say 105 km, shows the kind of spectrum, which is typical for electron excitation. These spectra are characterized by few and usually weak atomic lines, but strong bands particularly from nitrogen. The 1st positive group of nitrogen is greatly enhanced towards lower altitudes and the red ($N_2$1P) bands may be so intense at the lower limit as to give the auroral arc or band a deep red colour towards the bottom (Red aurora of type B due to electron excitation). Such spectrograms typical for electron excitation are characterised by a very weak red OI doublet, and sometimes it is hardly visible although other features are strong.

This indicates that the great enhancement of the red OI-doublet which leads to the red aurorae of type A, must be due to the positive ions contained in the neutralized bundle.

As we have found in previous papers and also in the present one, the enhancement of the OI doublet and the appearance of red aurorae of type A is usually accompanied by unusually intense hydrogen lines. This indicates that protons (and possibly other positive ions in the bundle) have a great ability for transferring the neutral OI atom from the ground states $^3P_{2,1}$ to the $^1D_2$-state, which is the upper state for the emission of the forbidden OI-doublet. This may possibly also apply to the enhancement of forbidden lines from OII, NI, NII and the N_2 ε-bands (V. K.-bands). (Cfr. paper 13, p. 46—48).

It may be of interest to notice that the two metastable OI-states: $^1D_2$ and $^1S_0$, correspond to excitation energies of 1,97 and 4,2 e. V. respectively, and that the corresponding electron velocities $0{,}9 \cdot 10^8$ and $1.2 \cdot 10^8$ cm/sec are of the same order of magnitude as the proton velocities, which we find from the auroral H Doppler effect. If the excitation of the metastable OI-states could be effected by slow electrons, the enhancement of the OI-doublet might be explained if most of the secondary electrons had velocities near $0.9 \cdot 10^8$ cm/sec (or a proper optimum) so that the population of the $^1D_2$-state was increased e. g. by resonance.

In a recent paper (19) M. J. Seaton tries to explain the effect of protons to excite the red OI-doublet by means of secondary electrons.

8. The properties of the neutralized bundles verified by «F»-spectrograms from Tromsø. The «F»-spectrograms taken at the Tromsø observatory during the winters 1953/54–1956/57 are reproduced on the five plates II–a, II–b, II–c, II–d and II–e. Each of these five plates is accompanied by a table «Explanation to the plate», containing the data, which are important for the evaluation of the consequences to be drawn from the spectrograms.

For the sake of convenience the necessary remarks regarding direction of the collimator and type of aurora is written on each copied spectrogram. On the spectrograms the H_α-lines are marked with a dot.

In order to see how the plates are going to be used, we may e. g. mention that the spectrograms with current numbers: 1, 2, 4, 5, 6, 7, 8, 9, 10 and 11 have at least been taken either towards south (S) or towards great altitudes and all of them show H_α-lines. The numbers 3, 12, 13, 14, 15 and 16 which have either been taken in the north direction or from altitudes near the lower limit, show no hydrogen effect (H_α).

On the five plates II we can distinguish between spectrograms mainly excited by electrons and those which are also in a marked degree excited by protons and perhaps other positive ions in the solar bundle.

The first type has comparatively strong bands of ($N_2$1P) and (N_2^+1N), a small number of lines and the red forbidden OI-doublets are much weaker than the green line (5577)– The second type has weak bands, relatively strong red OI-doublet and it shows a more or less strong H_α-line.

In the table 8 we have for each plate in one column (P) collected the spectrograms which are typical for positive ion-excitation, and in the second column (N) those which show the typical features of electron ray excitation.

Table 8. *Classification of spectrograms taken at Tromsø with the «F»-spectrograph. Reproduced on Pl. II-a to Pl. II-e.*

The columns (N): Spectrograms due to electron rays excitation near bottom edge.
— (P): Spectrograms from solar bundles with noticeable flux of pos. ions.
Spectrograms showing (H_α) are marked with a dot (·), w means weak. A means red aurorae of A-type. B means red aurora of the B-type.

Pl. II-a No		Pl. II-b No		Pl. II-c No		Pl. II-d No		Pl. II-e No	
P	N	P	N	P	N	P	N	P	N
1·	3	31·	33	57·	58	85·	86	107·A	108
2·	12	32·	35	61·	59	89·	87	109·A	113
4·	13	34·	36	64·	60	90·	88	110·A	119
5·	14	44·	37	65·	62	92·	91	111·	122B
6·	15	54·	41	68·	63	93·	95	114·	123B
7·	16	56·	42	72·	66	94·	96	115·	125
8·	18		43	74·	69	99·	97	116·A	126
9·	19		45	75·	70	100·	98	117·A	127
10·	20		46	82·	71	101·	102	118·A	130
11·	23		47		76	103·	104	120·	136
17·			48		77	106·	105	121·	138
21·			49		79			124·A	139
22·			50		80			128·A	
24·			51		81			129·W	
25·			52		83			132·A	
26·			53		84			133·A	
27·			55					135·	
28·									
29·									
30·									

The «F»-spectrograms on the plates II and the table 8 show that the auroral luminescence from near the bottom edge of ordinary aurorae is mainly due to electron-excitation and the H_α effect is absent.

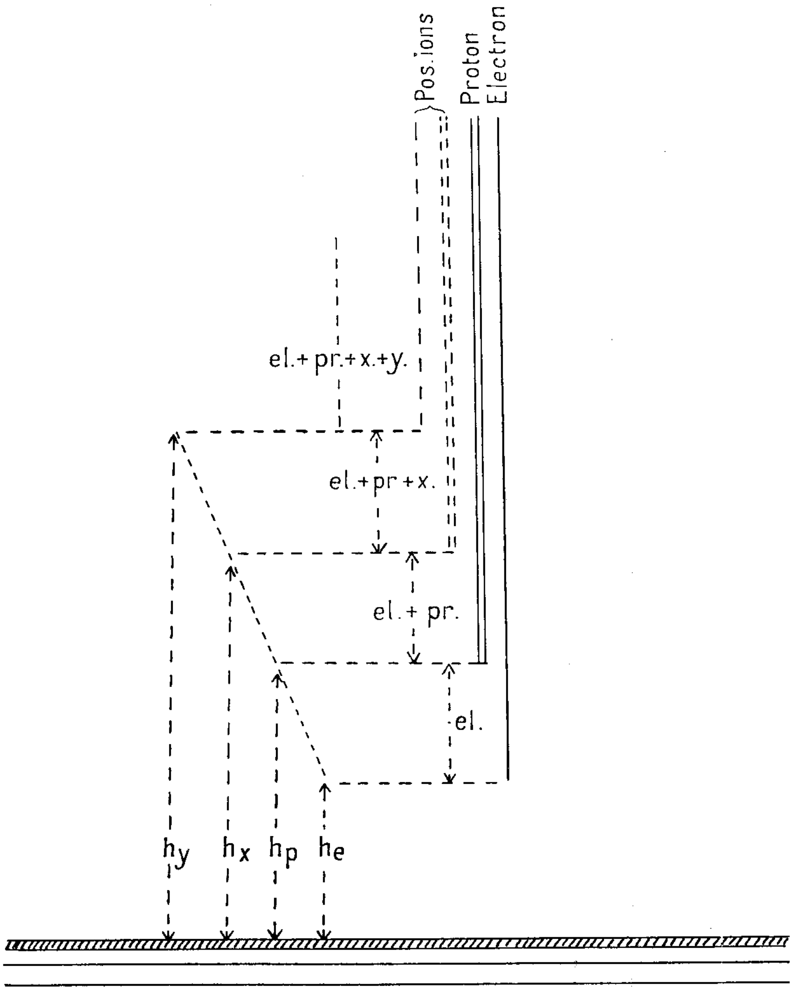

Fig. 3.

At some higher altitudes the effects of the positive rays of the bundle show up on the spectrograms. The effects are of two kinds: The emission from the protons, which have picked up electrons (indicated by H_α) and the effect of excitation of the atmospheric gases by the positive rays released from the solar bundle.

The separation of the electrons and the positive ions and their maximum range, when an originally neutralized bundle passes through the atmosphere, is illustrated by fig. 3.

All spectrograms in the column P of table 8 represent the spectral type, which is characteristic for positive ray excitation, and they show that the positive rays present in the neutralized bundle play a prominent part in the excitation of the auroral luminescence of these higher altitudes.

Most spectrograms in the P column also show the emission of H_α. Some exceptions however, are found in the P-column of the last plate II–e–. Two or three of the 10 spectrograms from red aurorae of type A and one other show no (H_α) effect. These exceptions may be due to the fact that the spectrograms in the P-group which show no H_α-line only contain the strong red forbidden OI-doublet and the green OI-line. The absence of H_α may only mean too small exposure.

The small intensity of H-lines compared with the great enhancement of the red OI-doublet would occur if the bundle were neutralized not merely with protons, but also with other positive ions capable of transfering the OI-atoms from the ($^3P_{2,1}$) state to the ($^1D_2$)-state. Such an excitation of the red OI-doublet may not be accompanied by the emission of H_α or any light which could be observed near the surface of the earth.

The F-spectrograms of the five plates II–a — II–e show that *the separation of the components of the neutralized bundle by the passage through the auroral region and the different range of the electrons, protons and other positive ions, has made it possible to analyse to a certain extent, the properties of each component separately. Thus we have found that in the lowest part between the stopping heights of the electrons* (h_e) *and the protons* (h_p) *the auroral luminescence is excited by electrons and shows the spectral type typical for electrons.* None of the protons or other positive ions in the bundle come down to this interval and no H_α effect from the proton rays of the bundle is observed in this interval. The spectrograms show no enhancement of the red OI-doublet by electron-excitation.

Only the spectrograms in the P-column corresponding to greater altitudes and greater flux of positive ions give an enhancement of the red OI-doublet, which may be great enough to give the aurorae a red colour of type A.

This means that the protons and perhaps other positive ions from the bundle, have the ability to produce a selective transfer of the OI-atom from the ground states ($^3P_{2,1}$) to the ($^1D_2$)-state.

Photometer curves from six «F»-spectrograms from red aurorae of type A are illustrated in paper 14 and relative intensities of the forbidden OI-lines and the H_α-line are given in table 1 of that paper (cfr. 14 p. 8 and 9).

It appears that the enhancement of the red OI-doublet in that case is accompanied by H_α, but there is no simple correspondence between the intensities of H_α and the OI-doublet. This probably means that there is no simple relation between the intensity of H_α and the flux of positive ions in the bundle.

The intensity of (H_α) is roughly proportional to the number of H_α-quanta emitted from unit length of the auroral streamers, which again in a complicated way depends on the proton flux in relation to the composition of the ionosphere at varying altitudes and to the form of the proton orbits.

The enhancement of the red OI-doublet, on the other hand, is essentially determined by the flux of the protons and other positive ions contained in the neutralized bundles.

Although there can be no strong correlation between the enhancement of the red OI-doublet and the intensity of H-lines, we have seen that the enhancement of the OI-doublet and the red aurorae of type (A) are due to the transition OI ($^3P_{2,1}$—$^1D_2$) effected by protons or perhaps also by other positive ions in the bundle.

Such a transition directly to the lowest metastable OI $^1D_2$-state is also interesting from a physical point of view. It must be left to those trained in quantum mechanics to find the theoretical solution of this excitation process.

Although no very direct correspondence between the intensity of H_α relative to the red doublet exists, we have tried to apply a statistical procedure. The intensities of H_α and the red OI-line 6300 were measured relative to that of the green line 5577, put equal to 100. The values of $I(H_\alpha)$ were divided into three intervals and the mean value inside each was found for the intensities of H_α and 6300. The results are shown in table 9.

Table 9.

Intervals $I(H_\alpha)$	0	0,1–5	5
$I(H_\alpha)$	0	2,7	12
I (6300)	21	48	153
Number of measurements	35	33	25

The table shows a marked increase in the relative intensity of the red OI-doublet with increasing mean value of H_α. The statistical correlation coefficient is about 0,5.

9. The Ionospheric temperature measured from «F»-spectrograms. The explanation of the terrestrial corona by means of X-rays from the sun was based on the low ionospheric temperatures measured by means of the intensity distribution of the rotational components of the R-branch of the negative bands of nitrogen.

Our measurements gave temperatures of about 40 → — 60° C. In our first measurements the temperature corresponded to altitudes of about 100—130 km. If, however, the slow decrease of density upwards was due to high temperature, it should have to increase upwards very rapidly and reach an order of magnitude of several thousand degrees at altitudes of say 200—300 km.

Spectrograms taken from the upper part of long auroral rays have not given any indication of an increase of temperature upwards (cfr. paper 18 p. 20 and paper 13 p. 49, 1950).

The great lightpower (F: 0,65) of the «F»-spectrograph has enabled us to obtain spectrograms from auroral rays at altitudes up to some hundred km.

Table 10. *Absolute Ionospheric Temperatures from «F» spectrograms.*

Spectrogram No	Band	T_π °K
Pl. II–a..... 1	4278	314
1	3914	306
3	4278	331
4	»	298
9	»	270
13	»	294
14	»	297
16	»	249
18	»	337
19	»	332
20	»	260
20	3914	239
21	4278	345
21	3914	304
26	4278	307
Pl II–b.....31	4278	327
34	»	311
35	3914	321
36	»	300
37	»	229
39	4278	295
40	»	289
42	»	309
46	»	305
46	3914	262
47	4278	297
47	3914	235
48	4278	356
49	»	333
50	»	350
51	»	352
52	»	372
53	»	321
55	»	324
56	»	363
Pl. II–c 57	4278	342
58	»	384
60	»	249
61	»	354
62	»	363
63	»	296
64	»	321
65	»	300
66	»	329
66	3914	243
71	4278	331
72	»	390
73	3914	287
74	4278	334
75	3914	293
78	»	235
79	4278	325
79	3914	231
81	4278	247
81	3914	224
82	4278	251
Pl. II–d.....87	4278	361
88	»	308
89	»	388
90	»	349
91	»	387
93	»	360
95	»	227
102	»	372
103	»	296
104	»	342
104	3914	272
105	4278	301
105	3914	289
106	4278	251

Mean T_π from band 4278 = 318.6°K
Mean T_π — 3914 = 266.9°K
Total mean T_π = 306.8°K

On account of small dispersion the overlapping of the rotational lines may produce errors, which tend to give too great values of the temperature. These errors, however, are very small compared with the great increase of temperature, which would be necessary to explain the slow rate with which the density within the auroral region diminishes towards greater altitudes.

The error due to overlapping or other errors due to the small dispersion, will be the same for the lower and the greater altitudes. For aurorae of the usual altitudes of 100 to 110 km, we have a great number of accurate temperature-measurements based on spectrograms taken with spectrographs of greater dispersion such as the «V»-spectrograph. The errors will depend on the adjustment of the spectrograph and the degree of exposure.

Some measurements, which were made by means of «F»-spectrograms during the winters 1951/52 and 52/53, were given in table XVII, paper 13, and the temperatures found agree well with those obtained from the «V»-spectrograms. The values found in paper 13 from the «F» spectrograms give no indication of increasing temperature with increasing altitude.

The temperatures found from some of the «F» spectrograms reproduced on the plates II–a, II–b, II–c and II–d are given in table 10. It appears that the temperatures found from these plates are usually too great.

In order to see if there is any increase of temperature towards greater altitude, we have found the mean of those at low altitude and compared them with the mean temperature from those spectrograms which correspond to the upper limit of auroral forms. The results are given in table 11.

Table 11.

Mean temperature		Number of bands
Lower limit	308°K	32
Top of aurorae	316°K	21

Within the limit of errors the temperatures are the same from the lower limit and from near the top of aurorae.

SPECTROGRAMS TAKEN AT OSLO WITH THE SPECTROGRAPHS (C) AND (a). CFR. TABLE 1.

10. Remarks regarding the type of spectrograms. From March 11. 1956 to January 22. 1957, we had 6 nights, when successful spectrograms were taken at Oslo. We had 4 nights in the spring and 1 in autumn of 1956 and one night 21—22 Jan. 1957.

The spectrograms from the spectrograph (C) are reproduced on pl. III and those from the (a) spectrograph on plate IV. To each plate follows an explanation.

In dealing with the Oslo spectrograms on the plates III and IV we must keep in mind the fact that the forbidden OI line 5577 and particularly the red OI-doublet 6300 and 6364 are greatly enhanced towards lower latitudes (19). Compared with the (N_2^+1N) band 4278 the intensity of the red OI doublet is on an average 3–4 times greater at Oslo than at Tromsø. We notice, that this enhancement-effect comes out very marked on all the Oslo spectrograms.

In addition to the latitude effect we have also to take into account the enhancement of the OI-doublet with altitude and the increase of sunspot activity.

In most cases the aurorae from Oslo consists of very long rays. From the height measurements of Størmer we learnt that the top of the rays went up to 600–700 km, so the length might amount to 450–550 km. Under such circumstances the spectral composition of the auroral luminescence is greatly influenced by proton excitation, which is essential for the appearance of H-lines.

The great enhancement of the red OI-doublet is seen from all spectrograms of the plates III and IV. On the (C) spectrograms taken on Kodak 103a–E the red OI-doublet and H_α are so strongly exposed that the two maxima are not always well separated on the copies, but are seen on the negative. On 15 of the spectrograms on plate III also the H_β-line can be seen. The photographic plates used for the (a) spectrograph (pl. IV) are not sensitive to H_α, but H_β can be seen on 12 of the 18 spectrograms. The absence of H_β may be due to weak exposure.

The enhancement of the red OI-doublet and the H-lines with increasing distance to the magnetic axis point confirms the existence of a close correlation between the red OI-doublet and the H-lines, which indicates that the protons have a great probability for transferring the OI-atoms from the ground state ($^3P_{2,1}$) directly to the $^1D_2$-state (cfr. papers 12, 13, 14).

11. Temperatures measured from the N_2^+1N bands obtained from the C-spectrograph. As already mentioned most of the aurorae, which were observed at Oslo in 1956–57 consisted of very long rays reaching altitudes of 600–700 km and spectrograms were taken corresponding to mean altitudes of up to 500 km. The (C) spectrograph has a dispersion smaller than that of the «F»-spectrograph and we cannot expect a very high accuracy of the measurements, but as the bands come out fairly sharp and and as most of them are taken at great altitudes, the accuracy may be sufficient to show if there is any great increase of temperature with increasing altitude.

The results of the temperature measurements are given in table 12. The numbers to the left refer to the spectrograms of plate III.

In the 5th column the measurements corresponding to average altitudes between 200–500 km are marked with H. Those corresponding to lower altitudes are denoted by L.

Table 12. *Ionospheric Temperatures observed at Oslo with the Spectrograph C.* The Spectrograms used are indicated by the numbers given in the Explanation to pl. III.

Pl. III No.	Date	Band	Temp K°	Altitude indication	Auroral type
1	11.3 56	3914	248	L	Lower part
3	2.3.56	4278	352	L	A, Lower part
5	17.4.56	»	310	L	A
6	»	»	301	H	Top R.
7	21–22–4–56	»	323	H	» R red type A
8	»	»	336	L	R et A.
9	»	3914	328	H	Red et R.
10	»	»	362	H	R
11	»	»	340	H	R and D.
13	26.10.56	4278	322	H	Top of R red
14	»	3914	299	H	Top R et B
17	21–22–1–57	4278	281	L	A
18	»	»	257	H	R et Cor.
20	»	»	245	H	Red et Cor.
24	»	»	285	H	Red type A.
27	»	»	270	L	D and R.

Mean H: 306°K
Mean L: 300°K } True temp. about 220°K

The mean value of the H-measurements = 306° K.
The mean value of the L-measurements = 300° K.

Thus there is no marked indication of any increase of ionospheric temperature with altitude and the true temperature corresponding to spectrograms of sufficiently great dispersion would be about 220° K.

12. The enhancement of spectral lines connected with excitation by great flux of protons and other positive ions in the neutralized bundle. From the spectrograms on plate III we notice that nearly all of them show features typical for excitation with positive rays. This means that the efficiency of the positive ions to excite luminescence showing strong lines, increases with altitude. It appears by a closer inspection, that most of the somewhat strongly exposed spectrograms show a number of enhanced features, mostly atomic lines. We may e. g. call attention to the spectrograms Nos. 1, 9, 10, 11, 12, 14, 22, 24, 25, 26. One of the spectrograms (No. 26) has been reproduced on a greater scale (fig. 4) and the enhanced features are indicated on the upper side of the spectrogram. Some of the stronger features have been measured and are given in table 13. The enhanced features are marked with a cross.

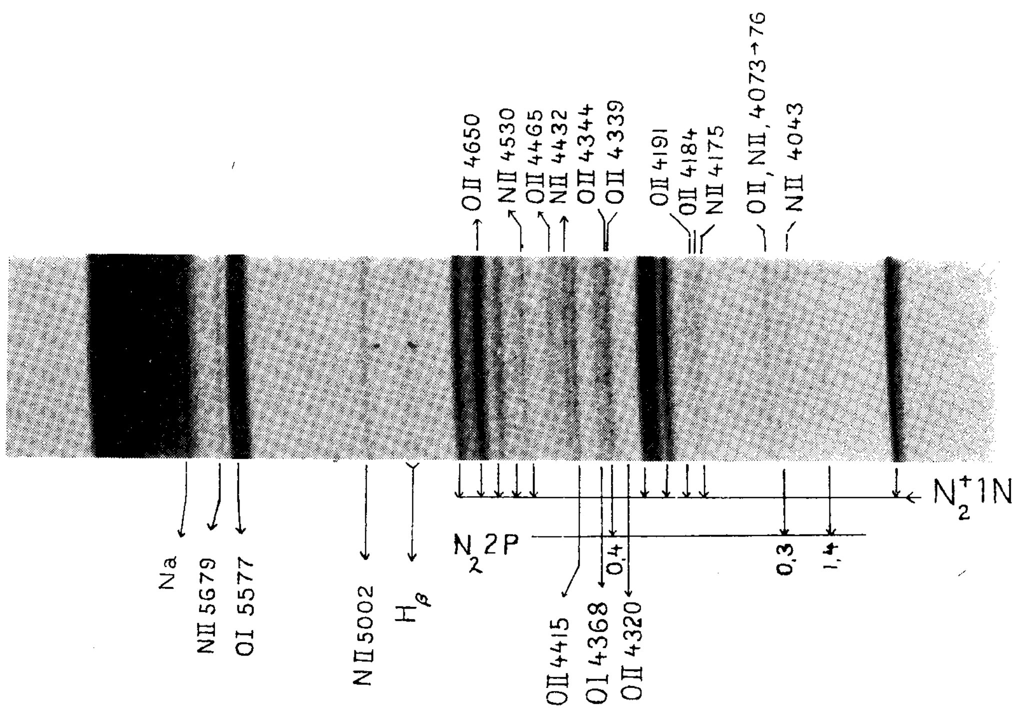

Fig. 4.

Table 13. *Enhanced Features (x) from a spectrogram taken at Oslo Jan. 21–22 1957 of red Aurorae of Type A.*

Features marked x usually absent.

λ	Interpretation	Intensity	Upper energy level e.v.
3914	N_2^+ 1N (0,0)	Strong	
3997	N_2 2P (1,4)	64	
4043 x	N II	44	26.2
4059	N_2 2P (0,3)	35	
4073 x	O II		28.7
4074 x	N II V.K. (2, 13)	51	26.2
4076	O II		28.7
4175	N_2^+ 1N (3, 4)	27	
4184 x	O II	23	31.3
4191	O II	26	31.3
4200	N_2^+ 1N (2, 3)	25	
4293	» (1, 2)	100	
4278	» (0, 1)	410	

Table 13. Continued.

λ	Interpretation	Intensity	Upper energy level e.v.
4320	O II	14	31.7
4339	O II	41	31.7
4344	N_2 2P (0.4)		31.7
4351	O II		28.5
4368	O I	39	12.4
4415	O II	45	26.2
4432 x	N II	35	26.2
4465 x	II O	27	33.2
4512	N_2^+ 1N (4, 6)	13	
4530 x	N II	29	26.2
4551	N_2^+ 1N (3, 5)	16	
4593	» (2, 4)	39	
4648	» (1, 3)	56	
		94	
4650 x	O II, V.K. (4, 16)	38	25.6
4709	N_2^+ 1N (0, 2)	87	
4843 x	V.K. (2, 15)		
4830—80	Hβ		
5002	N II	92	20,9—23,1
5577	O I	very strong	4.19
5679	N II	123	20.7

The extraordinary spectral intensity distribution of some Oslo spectrograms like No. 26 on plate III, can also be clearly seen by comparing it with a spectrogram taken with the same spectrograph at Oslo 8–9.3.1953. It was reproduced on the plate column A No. 6 of the paper 11 (G. P. vol. XIX No. 2, 1954).

The two spectrograms to be compared are shown on fig. 5, where some of the lines are indicated by numbers for which the interpretation is given in table 14.

As is apparent from previous papers and from the present one (cfr. § 8 and table 8) the spectrograms taken at Tromsø have shown that the auroral luminescence near the bottom edge is due to electron excitation. The H-lines did not appear and the red OI-doublets were either absent or weak. This means that the enhancement of the red OI-doublet is produced by protons (or other positive rays) contained in the neutralized bundle. In other words the protons (or possibly other positive ions) have a special facility for transferring the neutral OI-atoms from the normal OI-$^3P_{2,1}$-state to the lowest metastable state $^1D_2$.

In the case of the negative nitrogen bands (N_2^+1N) we see as a rule, that the intensities of the bands belonging to the same sequence will decrease with increasing quantnumber. Some of the Oslo spectrograms on plates III and IV seem to break this rule for the sequence n" – n' = 2, where the second band in the sequence N_2^+ 1N (1–3)

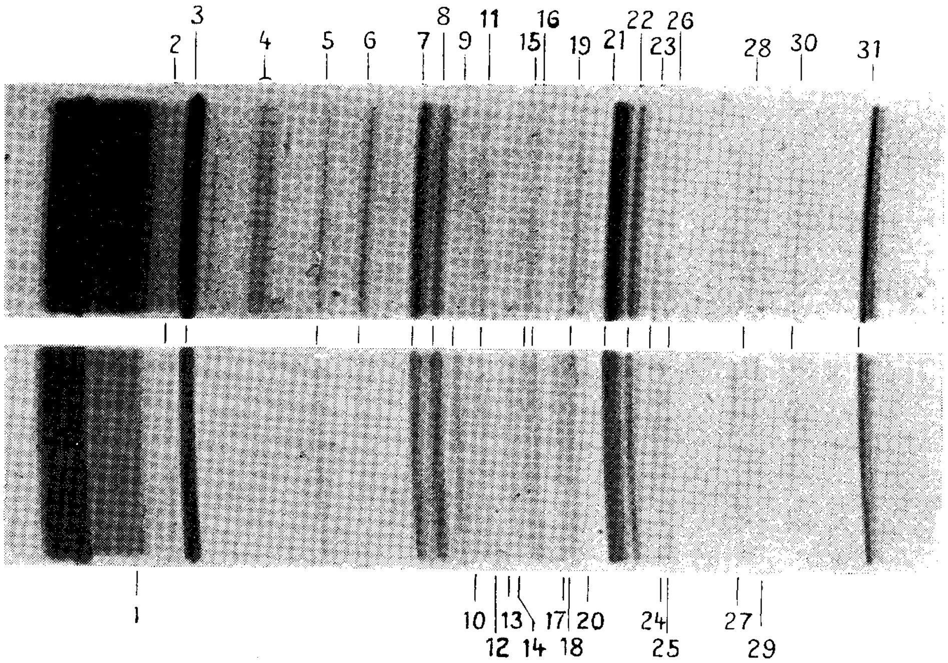

Fig. 5.

appears to be stronger than the first one N_2^+ 1N(o–2). This anomaly is very marked for some of the spectrograms taken during the night 21–22 January 1957. This irregularity is probably due to the enhancement of the OII-line 4650 or the N_2 V.K. (4,16) band. If we assume the latter feature has a relative intensity of say 38 and the N_2^+ 1N (1,3) band an intensity of 56, the sequence n = 2 will regain a normal fall of intensity with increasing quant number.

From the spectrograms on the plates III and IV we can see directly which of the two first bands of the sequence appears to be the stronger. On the spectrograms of plate III the 1st band of the sequence has the greatest intensity on the spectrograms Nos. 1, 3, 5, 6, 7, 8, 16 and the weakest one for Nos. 25, 26, 27, while they are about equally strong for the spectrograms Nos. 9, 10, 11, 12, 13, 15, 17, 18, 19, 22, 23, 24.

A similar result we obtained from the spectrograms on Plate IV taken with the small spectrograph (a) on Kodak 103 a–C.

The H_β-line on plate IV appears quite marked on the 12 somewhat strong spectrograms. The intensity of H_β is seen to vary considerably relative to other features e. g. the group of NII lines near 5002 Å. The intensity ratio $H_\beta/5002$ is greater than 1 for the spectrograms 2, 3, 5, 6, 8, 13 and 15, smaller than 1 for the spectrograms 7 and 16 and about equally strong on the spectrograms 8, 10 and 12.

The differences of the spectrograms from the spectrographs (C) and (a) are due

Table 14.

No. on fig. 5	Wavelength	Interpretation
1	5892	Na D_1, D_2
2	5679	N II
3	5577	O I
	5280—5200	O_2^+ 1N (2—0)
4		N_2^+ 1N (0—3) N I forbid.
5	5002	N II
6	4860	Hβ
7	4709	N_2^+ 1N (0—2)
8	4652	» (1—3) + O II. N_2V.K
9	4601	» (2—4)
10	4553	» (3—5)
11	4530	N II
12	4514	N_2^+ 1N (4—6
13	4490	» (5—7)
14	4465	O II
15	4432	N II
16	4415	O II
17	4368	O I
18	4358	O II
19	4340—35	N_2 2P (0—4)
20	4320	O II
21	4278	N_2^+ 1N (0—1)
22	4236	» (1—2)
23	4200	» (2—3
24	4191	O II
25	4184	O II
26	4175	N II
27	4076—73	O II. N II
28	4059	N_2 2P (0—3)
29	4043	N II
30	3997	N_2 2P (1—4)
31	3914	N_2^+ 1N (0—0)

to difference of instruments, photographic plates and different direction of the instrument on the sky.

All spectrograms from Oslo (plate III and IV) correspond to fairly great altitudes where the protons take an effective part in the excitation process. None of them is of the type which is typical for pure electron excitation.

Our thanks are due to Mr. A. Omholt for valuable help in the spectrographic work at Tromsø in the winter 1953/54 and to «Norges Almenvitenskapelige Forskningsråd» for financial support of the auroral investigations.

Oslo May 20th 1958.

REFERENCES

mainly dealing with the development of the explanation of solar-terrestrial relationships by means of X-rays.

1. L. VEGARD (L. V.): Theory of aurora and magn. disturbances founded on neutralized solar streams. Ann. d. Phys. IV, *50*, p. 583, 1916.

2. — The absorption of electrons and positive rays and the height and structure of aurorae. Phil. Mag. *42*, 47, 1921.

3. — The terrestrial and solar corona and the conductive ionized atmospheric layers explained through photo-electric effect of solar X-rays. a. Phil. Mag. 46, 193, 1923. b. C. R. *176*, p. 947, 1488, 1923.

4. — The solar electric bundles producing the aurorae and prominent magnetic disturbances are to be regarded as coronal streamers produced by photo-electric effects from X-rays originating from highly ionized matter in the sunspot region. Those bundles, like the streamers of the solar corona, are formed by photo-electrons neutralized by positive ions preferably protons. a. Det Norske vid. akad. Oslo, Skr. I No *2*, 1928. b. Geof. Publikasjoner (G. P.) Vol IX, No *11*, 1932. c. Physics of the earth. Edit by Fleming, Vol *VIII*, p. 573, written 1933. d. Ergebnisse d. exakt. Nat. wiss. Vol. *XVII*, p. 229, 1938.

5. — In 1939 and the next following years it was found that the auroral bundles emitted hydrogen lines showing Doppler effects corresponding to velocities up to (1—3) 10° cm/sec. This proves that the bundles consist of electrons neutralized by protons and possibly other positive ions. Regarding this discovery the following papers may be referred to:
   — a. Hydrogen showers etc. Nature *144*, p. 1089. 1939.
   — and E. TØNSBERG: b. Results of Auroral Spectrograms obtained at Tromsø 1941—42 and 1942—43. G. P. Vol *XVI*, No 2, 1944.
   — c. Proc. of the Brussels meeting of the Mixed Commis. of the Ionosphere, July 1948, p. 111. d. Phys. Soc. Gassiot Comm. Report p. 82, 1948. e. Trans. of the Oslo meeting of IUGG 1948, p. 189, 484. f. C. R. vol *230*, p. 1884 May 1950. g. Annales d. Geophys. Vol. *6*, p. 157, 1950. h. Transact. of the Congr. of IUGG at Brussels 1951.i. More detailed treatment of spectrograms showing Doppler effects obtained in the years 1940 to Feb. 1950 was given in G. P. *XVIII* No 5, 1952.

6. — and G. KVIFTE: G. P. *XVIII* No 3, 1951, Deal with Doppler effect on spectrogram from Feb. 1950.

7. A. B. MEINEL: Published spectrograms with H_{α}-Doppler effect. Nov. 1950. Astrophys. Journ. *112*, No 3, Nov. 1950.

8. C. W. GARTLEIN: Announce obs. of Doppler displacement of H_{α}. Phys. Rev. *81*, 103, p. 463, 1951.

9. L. VEGARD and E. TØNSBERG: G. P. *XVIII*, No 8, 1952. During the last years a great deal of work has been devoted to the verification of the consequences of the cosmical theories, particularly those connected with the solar electronic bundles, which are neutralized by positive ions (preferably protons), and we call attention to the following papers.

10. — Proceed. of the meeting of the Mixed Commis. of the Ionosphere at Canberra Aug. 1952 p. 135. The increase of proton flux towards lower latitudes.

11. — and G. KVIFTE: Theory and observations of the Enhancement of Auroral Hydrogen Lines with increasing distance from the Magnetic Axis Point. G. P. *XIX* No 2, 1954.

12. — Intensity Variations of Auroral Hydrogen Lines and influences of Solar Proton Radiation on the Auroral Luminescence. G. P. *XIX* No 4, 1954.

14. L. Vegard: Recent Progress relating to the study of Aurorae and Kindred Phenomena. G. P. *XX*, No 4, 1958.
13. — Composition, Variations and Excitation of the Auroral Luminescence Spectra. G. P. *XIX* No 9, 1956.
15. — The Temperature of the Aur. region etc. Terr. Magn. *37*, p. 389, 1932.
16. — and E. Tønsberg: Continued Investigations on the Temp. of the upper Atmosphere etc. G. P. *XI*, No. 2, 1935.
17. — Lichterscheinungen in Glimlicht und Kanalstrahlen. Ann. d. Phys. *IV*, 39. p. 111, 1912.
18. — G. P. Vol. *XII*, No 14, Table VII, 1940.
19. M. J. Seaton: J. Atm. Terr. Phys. *4*, 295, 1953.

Vol. XX.

Phenomena.

a. G. P. *XIX*

nosphere etc.

p. 111, 1912.

Explanation to Plate I–a and I–b.

Spectrograms taken at Tromsø with spectrograph «V».
Sort of plate: Kodak 103a–E, except spectr. Nos. 2 and 3 taken on 103a–F.

Sp. No.	Date	Exposure	Remarks on Aurora Type
1	12.10—27.10 53	5 h	Various forms
2	27.10—15.11	5 »	—
3	1. 2—10. 2 54	5—6 h	—
4	16. 2—25. 2	8 »	— Moonlight
5	26. 2— 7. 3	7 »	—
6	5.10—30.10	8 »	— Tow. N. h 10—20°
7	20.11–54–16.2.55	20 »	— Tow. Magn. Eq. N.
8	17. 2—25.4	7 »	Diff. Aur. + Corona tow. Magn. Z.
9	25.10—15.12	6 »	A and R
10	9. 1—18. 1—56	4 »	A, D, R. Foggy
11	30. 1—19. 2	10 »	D. R. A.
12	27. 2—22. 3	6 »	A, D, R. Weak red type A.
13	2.10—26.10	5½ h	D. R. red type A
14	9.11—56—4.1.57	10½ »	Red R type A, Pulsating, Foggy
15	24. 1— 4.3.	26 h	Red type A, R, D and A.

PLATE I–a

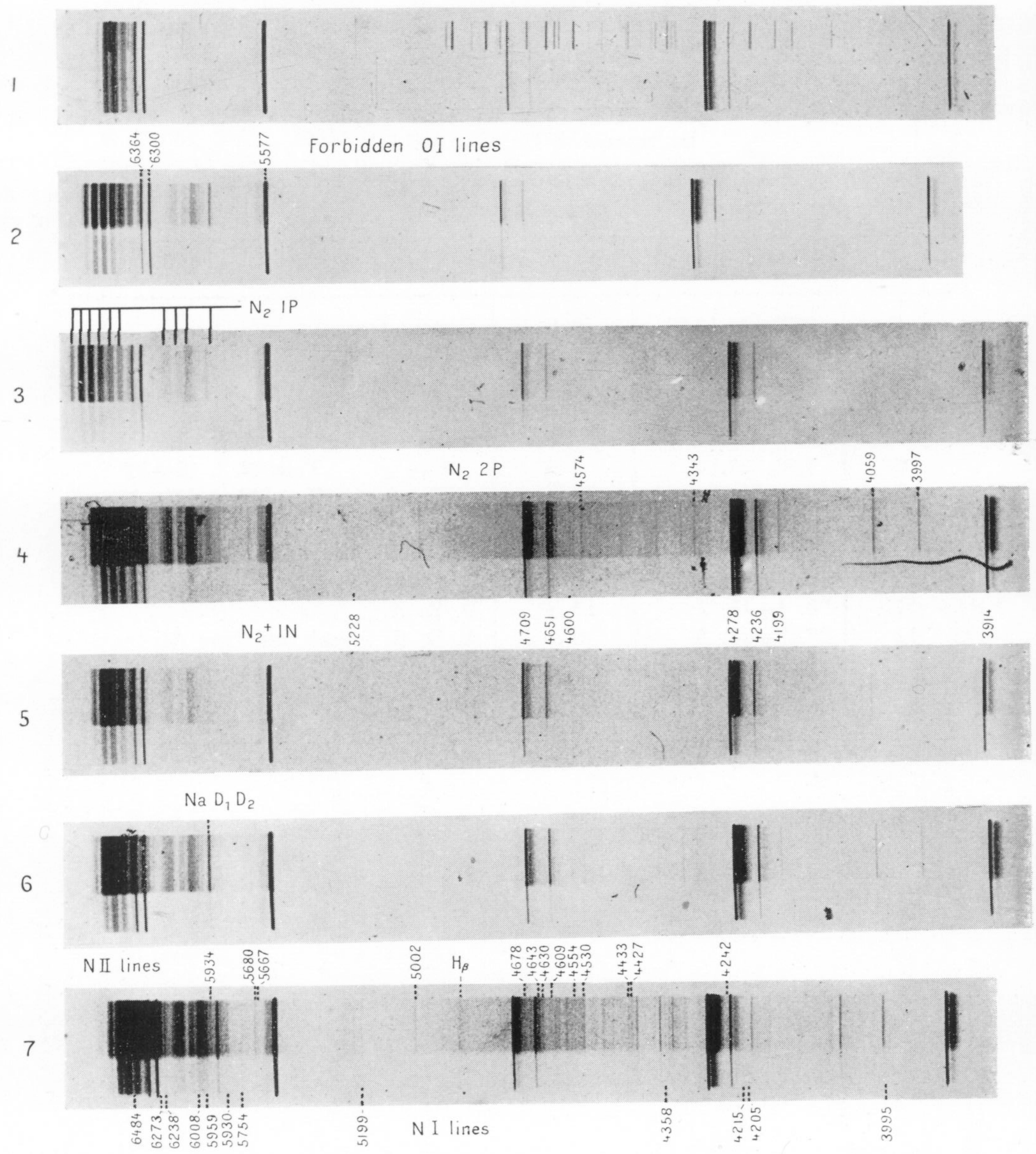

1
6364
6300
5577
Forbidden OI lines
2
N2 1P
3
N2 2P
4574
4343
4059
3997
4
N2+ 1N
5228
4709
4651
4600
4278
4236
4199
3914
5
Na D1 D2
6
NII lines
5934
5680
5667
5002
Hβ
4678
4643
4630
4609
4554
4530
4433
4427
4242
7
6484
6273
6238
6008
5959
5930
5754
5199
N I lines
4358
4215
4205
3995

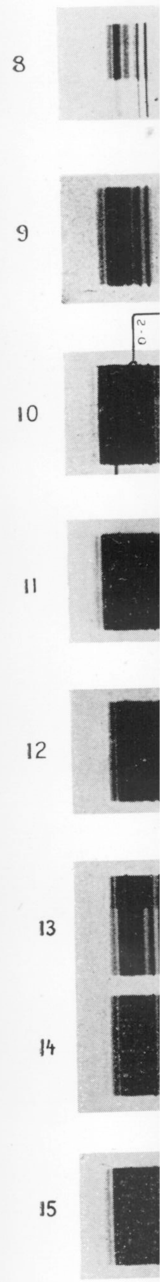

8
9
10
11
12
13
14
15

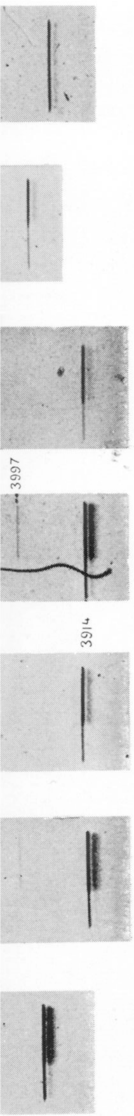
3997
3914

PLATE I–b

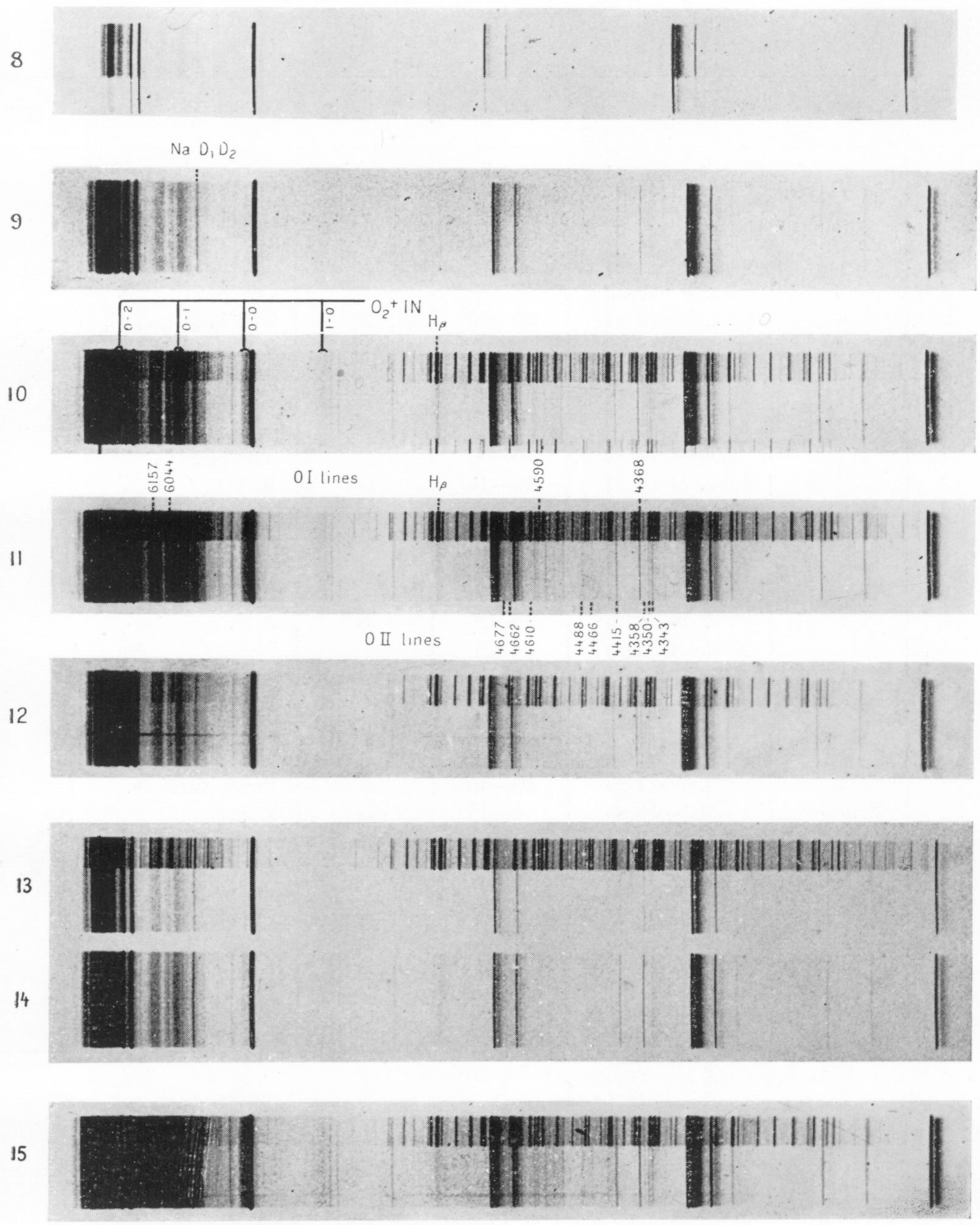
8
Na D1 D2
9
0-2
0-1
0-0
1-0
O2+ 1N
Hβ
10
6157
6044
OI lines
Hβ
4590
4368
11
4677
4662
4610
4488
4466
4415
4358
4350
4343
OII lines
12
13
14
15

Explanation to Plate II–a.

Spectrograms taken at Tromsø with spectrograph «F».

Sp. No	Date	Interval of Exposure	Height	Direction	Remarks on Auroral Type
1	16.10.1953	21.34—22.03	50—60°	S	Dif. surfaces
2	»	22.03—22.07	32°	S	Dif. A
3	»	22.08—22.16	12—15°	N—NW	D.
4	»	22.17—22.27	14°	S	Dif. A. L.
5	»	22.28—22.30		S	Dif. A. U.
6	»	22.30—22.34	60—90°	S	Top of R and C.
7	»	22.35—22.40	90°		C.
8	»	22.45—22.50	60—90°	S—SE	Top of R and C.
9	»	23.10—23.55	30°	S	W. dif. Aur.
10	17.10.	00.02—00.06	10°	S	R. A.
11	»	00.08—00.13	70—90°	S	Top of R.C.
12	»	00.27—00.33	13—14°	NW	R.A
13	27.10.	18.32—18.57	20—30°	S—SW	A.
14	»	18.58—19.17	30—35°	NW	A.
15	»	20.20—20.32	28°	N	A.
16	30.10.	21.25—21.50	15—30°	N	A and D.
17	»	21.51—22.35 (20.min. exp.)	18—20°	N	A.U.
18	1.11.	18.25—18.43	23°	N—NW	A.L.
19	»	18.47—19.05	80—90°	N—S	A.
20	»	19.05—19.10 (2½ min. exp.)	8—15°	N—NW	D.L.
21	»	19.20—21.30	30—40°	S	Foggy surfaces.
22	2.11.	19.02—20.05	8—15°	N	R.A.
23	3.11.	18.40—18.59	15°	N	A and D.
24	»	19.07—19.30	50°	N	Dif. Au. partly top of R.
25	»	19.32—20.18		N	A.
26	»	20.20—23.00		N	Various forms, w.
27	6.11.	19.10—19.33	10°	N	A, w.
28	»	19.34—20.05	20°	N	A.
29	»	20.06—20.49	75°	S	A, w.
30	»	20.50—22.00	45°	N	A.

Sort of Plate: 103a–E, except spectrogram 13–15, 103a–F.
Slit 55/100 mm except spectrogram 9, 15/100 mm.

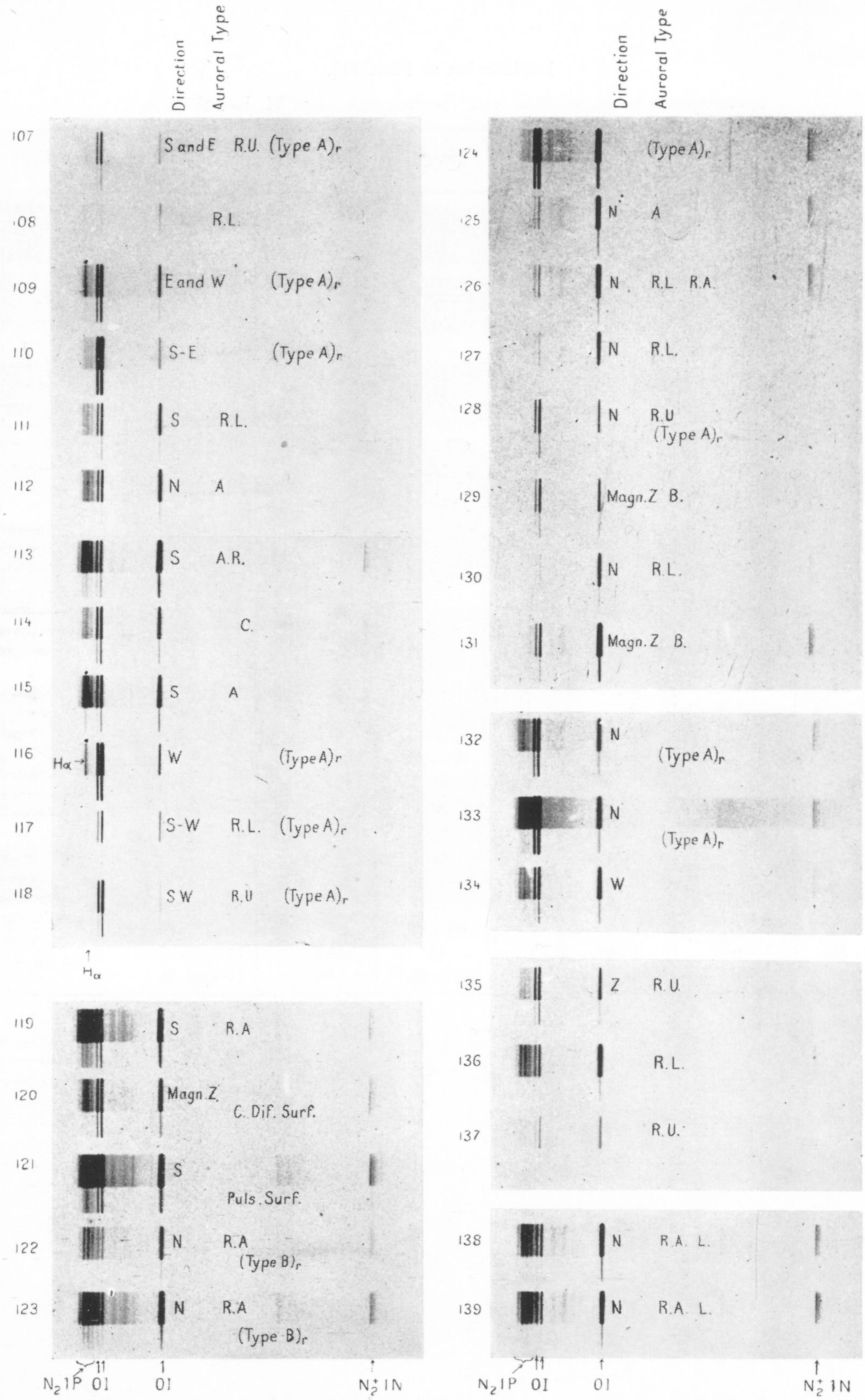
Direction
Auroral Type
107 S and E R.U. (Type A)r
108 R.L.
109 E and W (Type A)r
110 S-E (Type A)r
111 S R.L.
112 N A
113 S A.R.
114 C.
115 S A
116 Hα→ W (Type A)r
117 S-W R.L. (Type A)r
118 SW R.U (Type A)r
Hα
119 S R.A
120 Magn.Z C. Dif. Surf.
121 S Puls. Surf.
122 N R.A (Type B)r
123 N R.A (Type B)r
N2 1P OI OI N2+ 1N
Direction
Auroral Type
124 (Type A)r
125 N A
126 N R.L R.A.
127 N R.L.
128 N R.U (Type A)r
129 Magn.Z B.
130 N R.L.
131 Magn.Z B.
132 N (Type A)r
133 N (Type A)r
134 W
135 Z R.U.
136 R.L.
137 R.U.
138 N R.A. L.
139 N R.A. L.
N2 1P OI OI N2+ 1N

Explanation to Plate III.

Spectrograms taken at Oslo with spectrograph «C». Pl. Kodak 103a–E.

Sp. No.	Date	Interval of Exposure	Height	Direction	Remarks on Auroral Type
1	11.3. 1956	00.30—02.05	15—25°	N—NW	Lower limit D
2	»	02.05—02.25	47°	N—NW	Upper limit D
3	2—3.4.	23.30—01.55	15°	N	Lower limit A
4	»	01.55—02.45	32°	N—NE	Top R and A
5	17.4.	00.50—01.35	25°	N	A
6	»	01.35—02.30	50°	N—NW	Top R
7	21—22.4	22.27—22.47	60—80°		Top R. Red.
8	»	22.47—23.00	50°	N—NW	RA.
9	»	23.00—00.00		NE	Red surface and R
10	»	00.10—01.30			R
11	»	01.40—03.10	50—60°	NW	R and D
12	26.10.	21.30—22.30		E—NE	Red Surface and R
13	»	22.40—23.10			Top R and red surfaces
14	»	23.10—24.00	45°		Top R and B.
15	27.10.	01.35—02.35	35°	NW	Top R and Corona
16	»	02.35—03.00	25°	NW	R Lower limit.
17	21–22.1.57	20.00—20.25		N	A
18	»	20.30—21.00	80—90°		R and Corona
19	»	21.00—21.10	60°	W	Red Surfaces
20	»	21.10—21.30	70° and 90		Red Surfaces and Corona
21	»	21.38—21.46	28°	W	Red Surfaces
22	»	21.46—22.15	60°	NE	B.
23	»	22.30—23.05	80—90°		Top R, B and Corona
24	»	23.05—23.15	90°		Strong red Aurora
25	»	23.16—23.42	80—90°		Red Surfaces.
26	»	23.42—00.45	45°	W	D
27	»	01.00—01.17	60—80°	W	D and R.

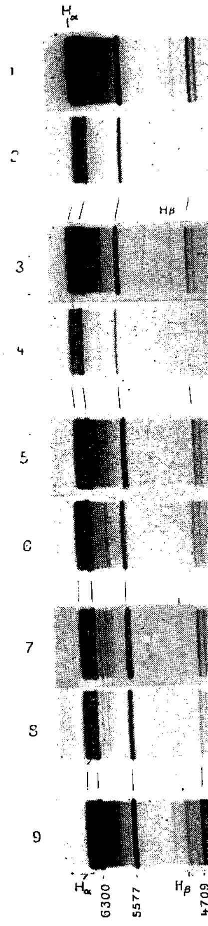

PLATE III

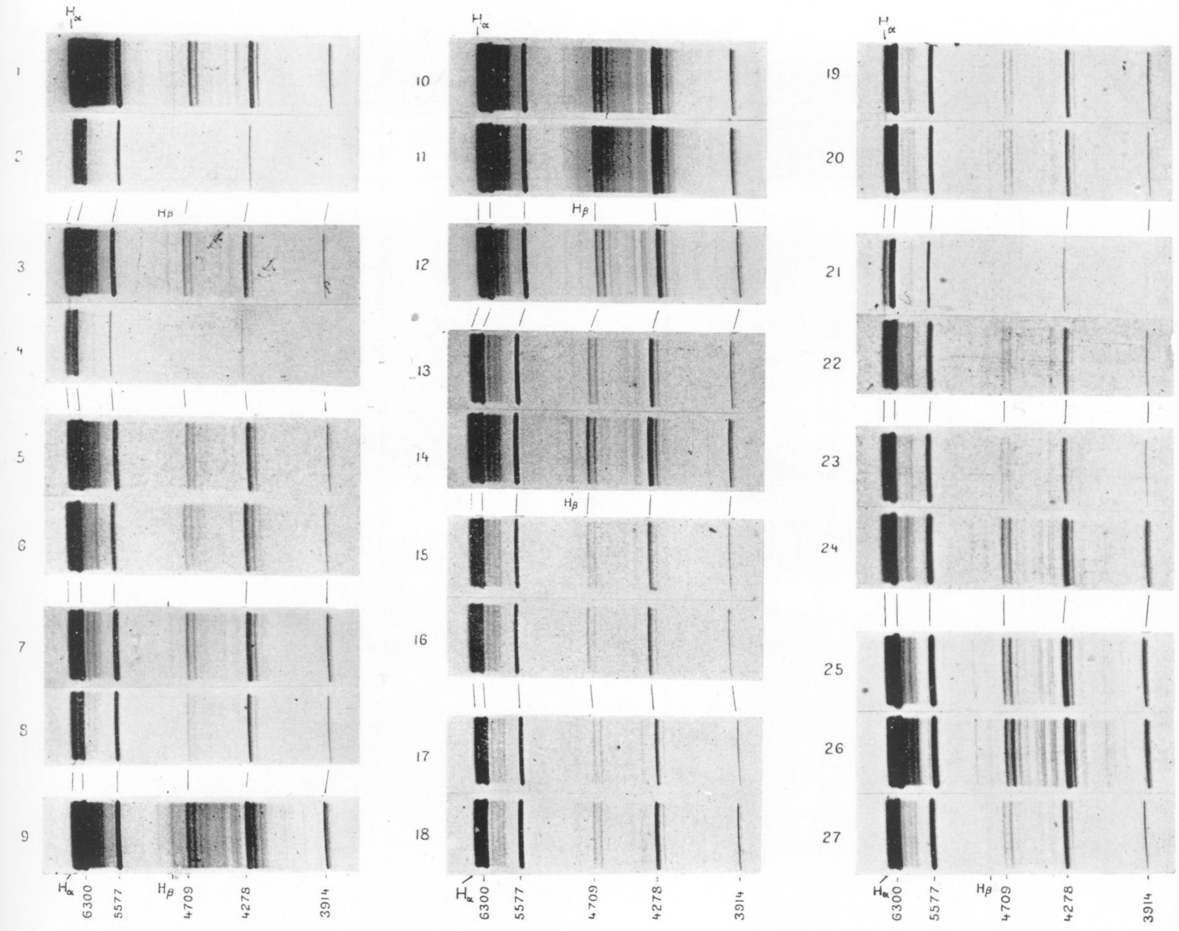

Hα
Hβ
1
2
3
4
5
6
7
8
9
10
11
12
13
14
15
16
17
18
19
20
21
22
23
24
25
26
27
6300
5577
4709
4278
3914

Explanation to Plate IV.

Spectrograms taken at Oslo with spectrograph «a».

Sp. No.	Date	Interval of Exposure	Height	Direction	Remarks on Auroral Type
1	11.3. 1956	00.45—01.25	40°	N—NW	Top R
2	»	01.25—02.25	15°	N—NW	R lower limit
3	2—3.4.	23.35—01.55	17°	N	A upper limit
4	»	01.55—02.45	13°	NW	A strongest part
5	21–22.4.	22.37—23.25		NNW	Various forms
6	»	23.25—01.30		W	Red surfaces and R
7	26.10.	21.50—22.35			Various forms
8	»	22.35—23.45		Magn. Z	Top R.
9	»	23.45—24.00			Top R
10	27.10.	02.00—02.40	25°	W	R
11	»	02.40—03.00	40°	W	Top R.
12	21.1. 1957	20.55—21.10			R & Corona
13	»	21.12—21.30	70° & Magn.Z		Red Aur.
14	»	21.38—21.46	28°	W	Red Aur.
15	»	21.46—22.15	60° Magn. Z.		Red surfaces.
16	»	23.05—23.16	Zenith		Strong red Aur.

Sort of Plate: Kodak 103a–C.
Slit: Spectrograms 1—6: 2/10 mm, 7—16: 3/10 mm.

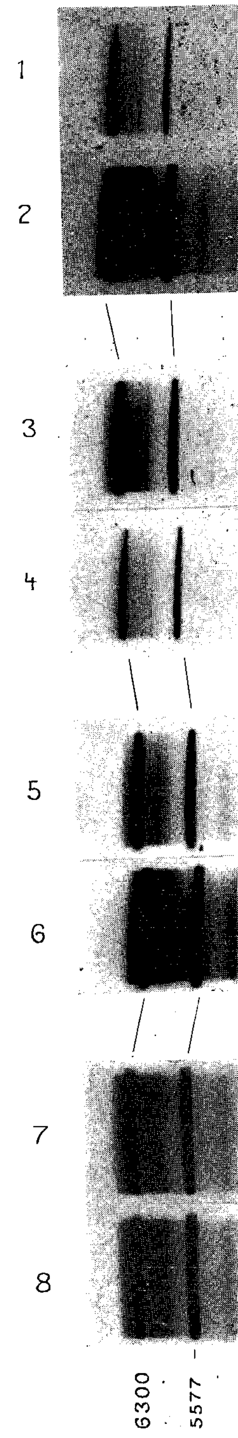

uroral Type

rt

nd R

r.

PLATE IV

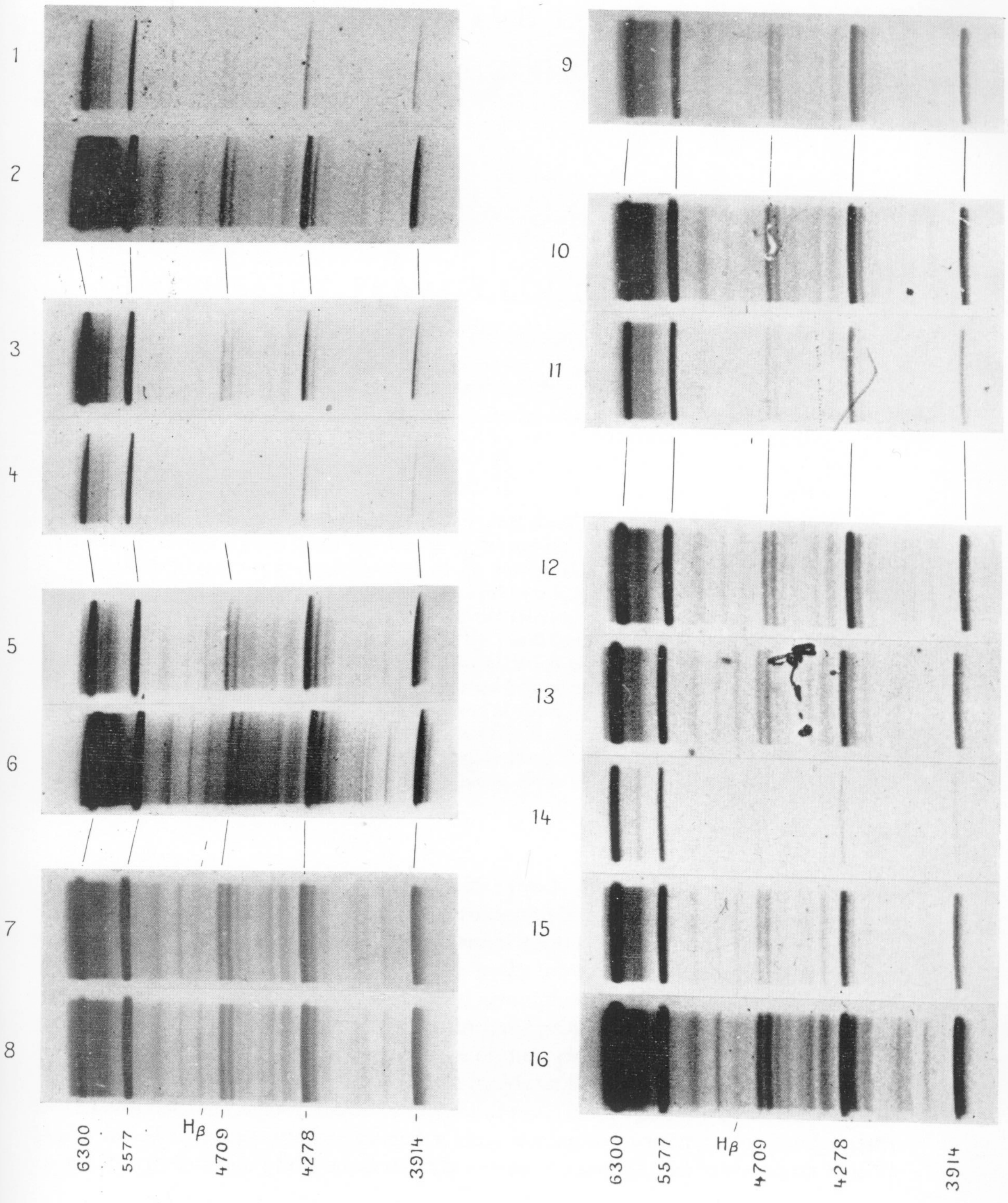

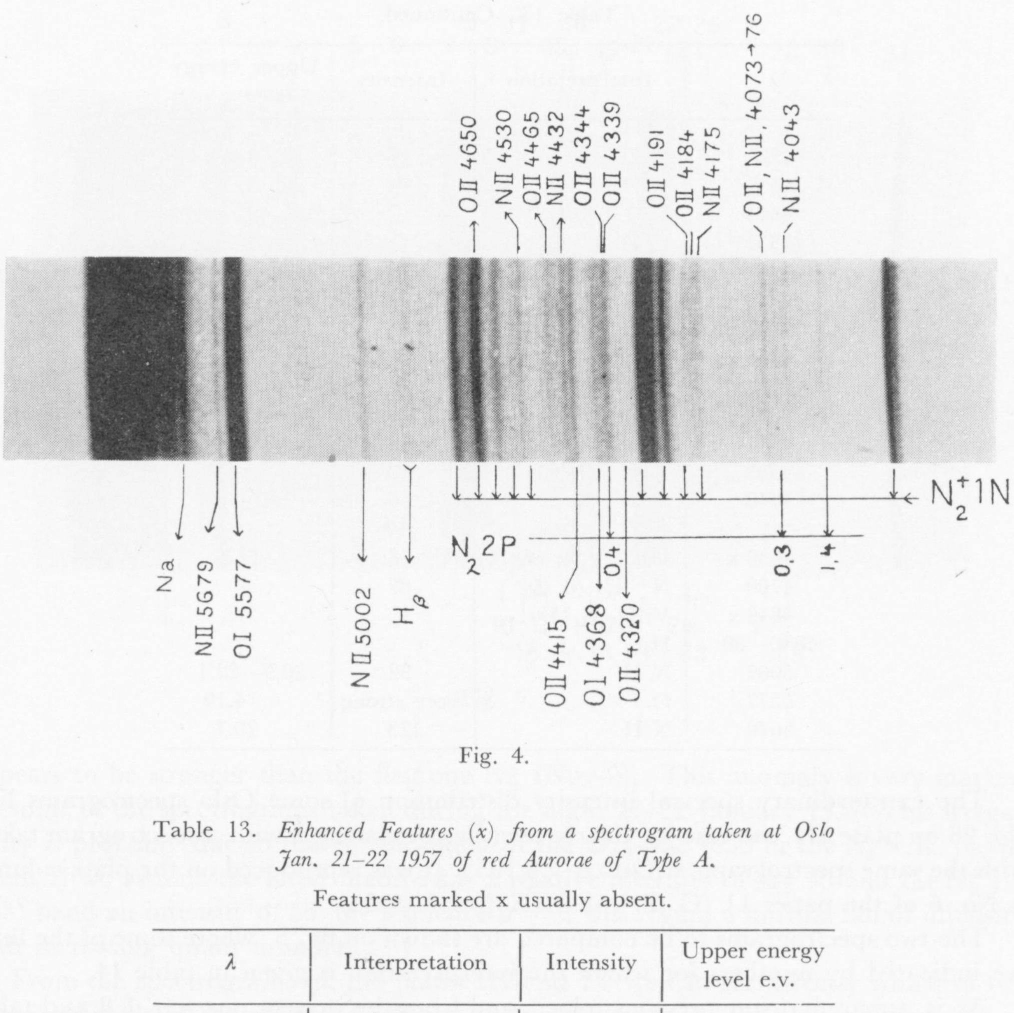

Fig. 4.

Table 13. *Enhanced Features (x) from a spectrogram taken at Oslo Jan. 21–22 1957 of red Aurorae of Type A.*

Features marked x usually absent.

λ	Interpretation	Intensity	Upper energy level e.v.
3914	N_2^+ 1N (0,0)	Strong	
3997	N_2 2P (1,4)	64	
4043 x	N II	44	26.2
4059	N_2 2P (0,3)	35	
4073 x	O II		28.7
4074 x	N II V.K. (2, 13)	51	26.2
4076	O II		28.7
4175	N_2^+ 1N (3, 4)	27	
4184 x	O II	23	31.3
4191	O II	26	31.3
4200	N_2^+ 1N (2, 3)	25	
4293	» (1, 2)	100	
4278	» (0, 1)	410	

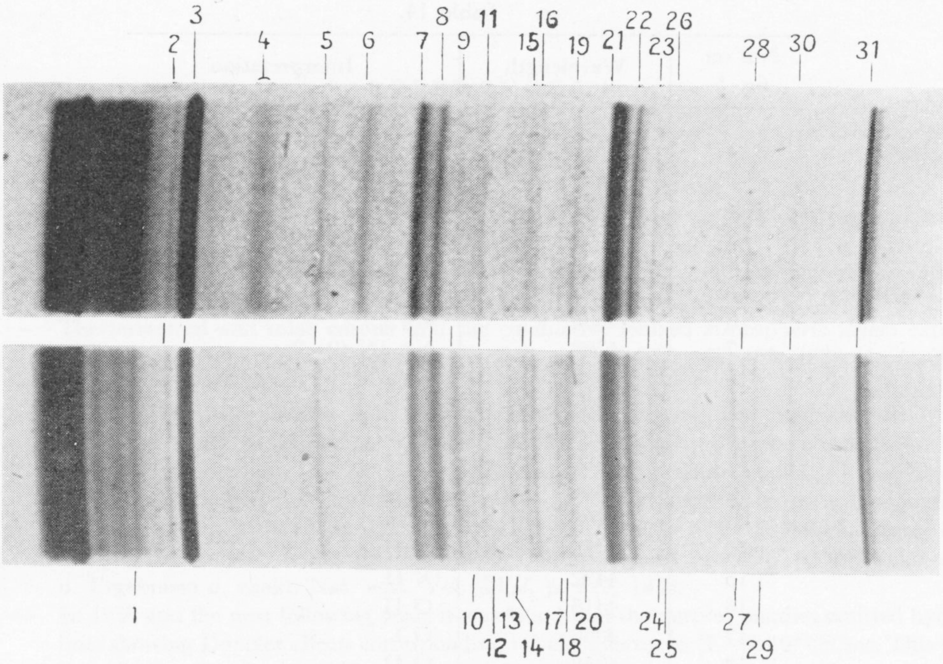

Fig. 5.

appears to be stronger than the first one N_2^+ 1N(o–2). This anomaly is very marked for some of the spectrograms taken during the night 21–22 January 1957. This irregularity is probably due to the enhancement of the OII-line 4650 or the N_2 V.K. (4,16) band. If we assume the latter feature has a relative intensity of say 38 and the N_2^+ 1N (1,3) band an intensity of 56, the sequence $n = 2$ will regain a normal fall of intensity with increasing quant number.

From the spectrograms on the plates III and IV we can see directly which of the two first bands of the sequence appears to be the stronger. On the spectrograms of plate III the 1st band of the sequence has the greatest intensity on the spectrograms Nos. 1, 3, 5, 6, 7, 8, 16 and the weakest one for Nos. 25, 26, 27, while they are about equally strong for the spectrograms Nos. 9, 10, 11, 12, 13, 15, 17, 18, 19, 22, 23, 24.

A similar result we obtained from the spectrograms on Plate IV taken with the small spectrograph (a) on Kodak 103 a–C.

The H_β-line on plate IV appears quite marked on the 12 somewhat strong spectrograms. The intensity of H_β is seen to vary considerably relative to other features e. g. the group of NII lines near 5002 Å. The intensity ratio $H_\beta/5002$ is greater than 1 for the spectrograms 2, 3, 5, 6, 8, 13 and 15, smaller than 1 for the spectrograms 7 and 16 and about equally strong on the spectrograms 8, 10 and 12.

The differences of the spectrograms from the spectrographs (C) and (a) are due